



MASTER THESIS

TECHNICAL MEDICINE

Accuracy, reliability, and applicability of electrical cardiometry for measuring cardiac output in critically ill newborns

Chantal Lokhorst

Examination committee

Chair: Prof. dr. D.W. Donker

Medical supervisor: Prof. dr. W.P. de Boode

Technological supervisor: Dr. E. Mos-Oppersma

Process supervisor: Dr. M. Groenier

External member: D. Van Dartel, MSc.

Additional members: Dr.ir. B.E. Westerhof & Dr. R. van der Lee

October 2021

ABSTRACT

Background & objective: Patients admitted to a neonatal intensive care unit (NICU) are (continuously) monitored on heart rate, blood pressure, arterial oxygen saturation, and biochemical parameters. To assess the haemodynamic state more accurately, cardiac output (CO) should also be taken into consideration, as this can assist in timely recognition of hypoperfusion and early stages of shock. Measuring CO in neonates is complex, as most of the methods used in adults cannot be applied in neonates. Electrical cardiometry (EC) is a method based on bioimpedance that continuously measures CO. Research validating EC in (preterm) neonates is scarce. Therefore, the aim of this study is to determine the accuracy of EC to measure CO in critically ill neonates, using transthoracic echocardiography (TTE) as a reference method.

Methods: Patients admitted to the NICU of the RadboudUMC Nijmegen, the Netherlands, with a gestational age between 26 and 42 weeks were included. CO was continuously measured with EC (CO_{EC}) and TTE was performed at least once per day to obtain left and right ventricle output (LVO_{TTE} , RVO_{TTE}). Bland-Altman analysis was performed to determine the agreement between the two methods and trending ability was assessed using concordance and polar plot analysis.

Results: 43 echocardiography's were performed in 19 neonates with a median (IQR) gestational age of 29.4 (28.1 – 31.0) weeks and a weight of 1109 (983.5 – 1380) g. Mean \pm SD of CO_{EC} , LVO_{TTE} , and RVO_{TTE} was 224 ± 40 , 244 ± 98 , and 335 ± 112 mL/min/kg, respectively. Bland-Altman analysis of CO_{EC} and LVO_{TTE} [RVO_{TTE}] resulted in a mean bias and precision ($1.96 \times SD$) of -19.6 [-110.3] and 212 [212.5] ml/min/kg, respectively, with a percent bias of -8% [-32.9%] and a percent error of 81.6% [55.9%]. For trending ability, the concordance rate was 55.5% [50%] and the angular bias \pm radial limits of agreement was $-29.5^\circ \pm 60^\circ$ [$23.6^\circ \pm 60^\circ$].

Conclusion: There was no interchangeability between EC and TTE. Since echocardiography has its limitations and a percent error of 30%, it is unclear to what extent the disagreement between the two methods is caused by erroneous CO measurements of either EC or TTE. This emphasizes the need for another, more accurate reference method.

LIST OF ABBREVIATIONS AND ACRONYMS

3D	3-dimensional
AV	Arteriovenous
CO	Cardiac output
COV	Coefficient of variation
CSA	Cross sectional area
DA	Ductus arteriosus
EC	Electrical cardiometry
FO	Foramen ovale
HR	Heart rate
IQR	Interquartile range
LOA	Limits of agreement
LVO	Left ventricular output
LVOT	Left ventricular outflow tract
LVSV	Left ventricular stroke volume
nCPAP	Nasal continuous positive airway pressure
NICU	Neonatal intensive care unit
PA	Pulmonary artery
PDA	Patent ductus arteriosus
PFO	Patent foramen ovale
RVO	Right ventricular output
RVOT	Right ventricular outflow tract
RVSV	Right ventricular stroke volume
SD	Standard deviation
SpO ₂	Oxygen saturation
SQI	Signal quality index
SV	Stroke volume
TPUD	Transpulmonary ultrasound dilution
TTE	Transthoracic echocardiography
VTI	Velocity time integral

TABLE OF CONTENTS

- Abstract** i
- List of abbreviations and acronyms** iii
- List of figures** viii
- List of tables** ix
- 1 Introduction** 1
- 2 Theoretical framework** 3
 - 2.1 Transitional haemodynamics 3
 - 2.2 Clinical relevance of haemodynamic monitoring 3
 - 2.3 Technological aspects of cardiac output monitoring 5
 - 2.3.1 Transthoracic echocardiography 5
 - 2.3.2 Electrical cardiometry 7
- 3 Aim** 11
- 4 Methods** 13
 - 4.1 Population and study design 13
 - 4.2 Data acquisition 13
 - 4.3 Data analysis 14
 - 4.3.1 Validation of electrical cardiometry 14
 - 4.3.2 Trending ability of electrical cardiometry 15
 - 4.3.3 Heart rate comparison 16
 - 4.3.4 Influence of patient weight and height 16
 - 4.3.5 Influence of transthoracic echocardiography 16
 - 4.3.6 Usability: durability of electrodes 17
- 5 Results** 19
 - 5.1 Population 19
 - 5.2 Validation of electrical cardiometry 19
 - 5.3 Trending ability of electrical cardiometry 22
 - 5.4 Heart rate comparison 24
 - 5.5 Influence of patient weight and height 26
 - 5.6 Influence of transthoracic echocardiography 26
 - 5.7 Usability 30
- 6 Discussion** 33
 - 6.1 Validation and trending ability of electrical cardiometry 33
 - 6.2 Reliability 34
 - 6.3 Usability 35

6.4 Limitations	35
7 Conclusion	37
8 Recommendations and future work	39
References	40
Appendix A: Figures	45
Appendix B: Tables	47

LIST OF FIGURES

2.1 Schematic representation of the fetal circulation (left) with the foramen ovale and the ductus arteriosus which turn into the fossa ovalis and the ligamentum arteriosum in the neonatal circulation (right). Adapted from [1] 4

2.2 Schematic representation of pulsed-wave Doppler. With Δf : Doppler shift; f_t : frequency of transmitted signal; f_r : frequency of received signal; θ : angle of insonation; v : velocity and RBCs: red blood cells. Adapted from [2] 6

2.3 Example of LVO measurement with TTE. Reprinted with permission from [3] 7

2.4 Example of RVO measurement with TTE. Reprinted with permission from [3] 8

2.5 Explanatory figure of the EC theory. At the top, the ECG signal is shown. The inverted change of impedance (middle, $-dZ(t)$) increases upon opening of the aortic valve and decreases during diastole. The peak in the calculated time-derivative of $-dZ(t)$ (bottom, $-\frac{dZ(t)}{dt}$) corresponds to the peak aortic acceleration. LVET: left ventricular ejection time; T_{RR} : R-R interval. Adapted from [4] 9

4.1 Representation of the electrode positions on a (premature) baby mannequin. A: right temporal area; B: right side of the neck; C: left midaxillary line at xiphoid level; D: left inner thigh. 13

4.2 Timeline of the intervals used to determine the influence of TTE on the haemodynamic parameters and SQI. 17

5.1 Bland-Altman analysis of CO_{EC} and LVO_{TTE} (N = 43). 20

5.2 Bland-Altman analysis of CO_{EC} and RVO_{TTE} (N = 41). 20

5.3 Scatter plot of CO_{EC} and LVO_{TTE} with marked regions for categorisation (N = 43). Blue: low CO (<150 mL/min/kg); green: normal CO (150-350 mL/min/kg); red: high CO (>350 mL/min/kg). 21

5.4 Scatter plot of CO_{EC} and RVO_{TTE} with marked regions for categorisation (N = 41). Blue: low CO (<150 mL/min/kg); green: normal CO (150-350 mL/min/kg); red: high CO (>350 mL/min/kg). 21

5.5 Concordance plot of CO_{EC} and LVO_{TTE} with an exclusion zone (in grey) of 30 mL/min/kg (N = 24). The dashed line represents the angle of identity. 22

5.6 Concordance plot of CO_{EC} and RVO_{TTE} with an exclusion zone (in grey) of 30 mL/min/kg (N = 22). The dashed line represents the angle of identity. 23

5.7 Polar plot of CO_{EC} and LVO_{TTE} with an exclusion zone of 20 mL/min/kg (N = 24). The dotted line represents the angular bias (-29.5°) and the dashed lines represent the radial limits of agreement (30.5° & -89.5°). 23

5.8 Polar plot of CO_{EC} and RVO_{TTE} with an exclusion zone of 20 mL/min/kg (N = 22). The dotted line represents the angular bias (-23.6°) and the dashed lines represent the radial limits of agreement (36.4° & -83.6°). 24

5.9 The cross-covariance between HR_{EC} and reference method HR_{ECG} 25

5.10 HR data of a single patient over time along with the SQI. At the top, the original HR_{EC} and HR_{ECG} is shown. At the bottom, the HR_{ECG} data is shifted forward for the obtained lag of 1 minute.	25
5.11 Difference between HR_{EC} and HR_{ECG} of a single patient over time. At the top, the original HR_{EC} and HR_{ECG} is shown. At the bottom, the HR_{ECG} data is shifted forward for the obtained lag of 1 minute.	26
5.12 Correlations and lines of regression between patient weight or height and CO. A: weight vs CO_{EC} (N = 43); B: height vs CO_{EC} (N = 43); C: weight vs LVO_{TTE} (N = 43); D: height vs LVO_{TTE} (N = 43); E: weight vs RVO_{TTE} (N = 41); F: height vs RVO_{TTE} (N = 41).	27
5.13 Measured parameters of a single patient for the three intervals; before, during, and after TTE.	29
5.14 The proportion of samples with a good SQI ($\geq 70\%$) over time shown for three individual subjects.	31
1 Bland-Altman analysis of SV_{EC} and $LVS_{V_{TTE}}$ (N = 43).	45
2 Bland-Altman analysis of SV_{EC} and $RVS_{V_{TTE}}$ (N = 41).	45
3 Measured diameter of the LVOT at the hinge points of the aortic valve in patients where multiple TTE's were performed (N = 13).	46
4 Measured diameter of the RVOT at the pulmonary valve insertion in patients where multiple TTE's were performed (N = 13).	46

LIST OF TABLES

2.1	Validation studies of EC. NA: not available.	10
5.1	Patient demographics (N=19).	19
5.2	Results of the Friedman's ANOVA tests with the effect size expressed by Kendall's W (N = 41). * SQI < 70%	28
1	Results of the Bland-Altman analyses of HR_{EC} and HR_{ECG} (N = 19).	47
2	Results of the Bland-Altman analyses of HR_{EC} and HR_{ECG} , with HR_{ECG} shifted for the time lag (N = 19).	47

1 INTRODUCTION

Each year approximately 4,000 neonates are admitted to one of the nine neonatal intensive care units (NICUs) in the Netherlands.^[5] This number includes both term and preterm (born before 37 weeks of gestation) neonates with various conditions, such as cardiovascular problems, respiratory problems, or congenital disorders. Patients admitted to the NICU are monitored on several clinical and biochemical parameters, which can be used by the physicians to estimate cardiac output (CO). However, the clinical estimation of CO is unreliable as research in a paediatric intensive care setting has shown that only 26% of the patients in a true low CO state are correctly categorized as such.^[6] If the low CO state is not recognised in time, the systemic hypoperfusion and early stages of shock can progress to uncompensated shock, leading to increased morbidity and mortality. Hence, monitoring of the CO should also be taken into consideration to determine the hemodynamic state of the infant more accurately. Unfortunately, measuring the CO in neonates is complex, as most of the methods used in adults cannot be applied in neonates due to technical limitations. Several systems to monitor the CO have been brought to market over the last few years, but evidence supporting their use and reliability in (preterm) neonates is lacking.^[7, 8, 9] This study therefore seeks to examine the usefulness of one of many noninvasive electrical biosensing technologies to measure the CO in critically ill (preterm) neonates.

2 THEORETICAL FRAMEWORK

2.1 Transitional haemodynamics

At birth, a major transition in haemodynamics takes place when the foetal circulation changes into the neonatal circulation (see Figure 2.1). In utero, gas exchange occurs in the placenta from which the oxygen-rich blood flows through the umbilical vein into the inferior vena cava via the ductus venosus. Upon entering the right atrium, most of the blood is shunted through the foramen ovale (FO) to the left atrium, from where it flows into the left ventricle and aorta. The ductus arteriosus (DA) allows the blood that entered the right ventricle and pulmonary artery (PA) to shunt directly into the aorta, so it can bypass the high-resistance pulmonary system. Because of the right-to-left shunts, the right ventricle is accountable for 65% of the combined ventricular CO.^[7]

As soon as the infant takes its first breath, pulmonary vascular resistance decreases, while systemic vascular resistance increases due to cord clamping. The decreased pulmonary vascular resistance allows an increase of the pulmonary blood flow, and more blood enters the left atrium, leading to an increase of left atrial pressure, which causes functional closure of the FO. After a few weeks, the FO is permanently closed and forms the fossa ovalis. DA closure is initiated by withdrawal of prostaglandin production, and it contracts due to an increase of arterial oxygen content. The DA physiologically closes within 24 hours after birth in term neonates and complete closure occurs within a month, after which it turns into the ligamentum arteriosum.^[7] In preterm neonates born at or after 30 weeks of gestation, a patent ductus arteriosus (PDA) is seen in 10% and 2% of the cases by respective 4 and 7 days after birth.^[10] 79% and 66% of the extremely preterm infants born between 25 and 28 weeks of gestation have a PDA by respective 4 and 7 days after birth.^[10] The majority of the infants with a PDA show left-to-right shunting.^[7] When ductal and interatrial shunts are absent, left ventricular output (LVO) and right ventricular output (RVO) reflect systemic blood flow and systemic venous return, respectively. In the presence of left-to-right shunting through a PDA, LVO overestimates systemic circulation, and systemic venous return is overestimated by RVO when left-to-right shunting occurs through a patent foramen ovale (PFO).^[3]

2.2 Clinical relevance of haemodynamic monitoring

Nowadays, neonates are haemodynamically monitored by (continuous) measurements of the heart rate (HR), arterial oxygen saturation (SpO₂), blood pressure, capillary refill time, urine output, serum lactate concentration, blood gas analysis, and central-peripheral temperature difference. However, these parameters show poor correlation with systemic blood flow. A more reliable determinant of systemic blood flow, and therefore also of oxygen delivery, is the CO. This is the amount of blood pumped by the heart per minute and is given by the product of the HR and the stroke volume (SV), which in turn is determined by preload, contractility, and afterload.^[8, 9]

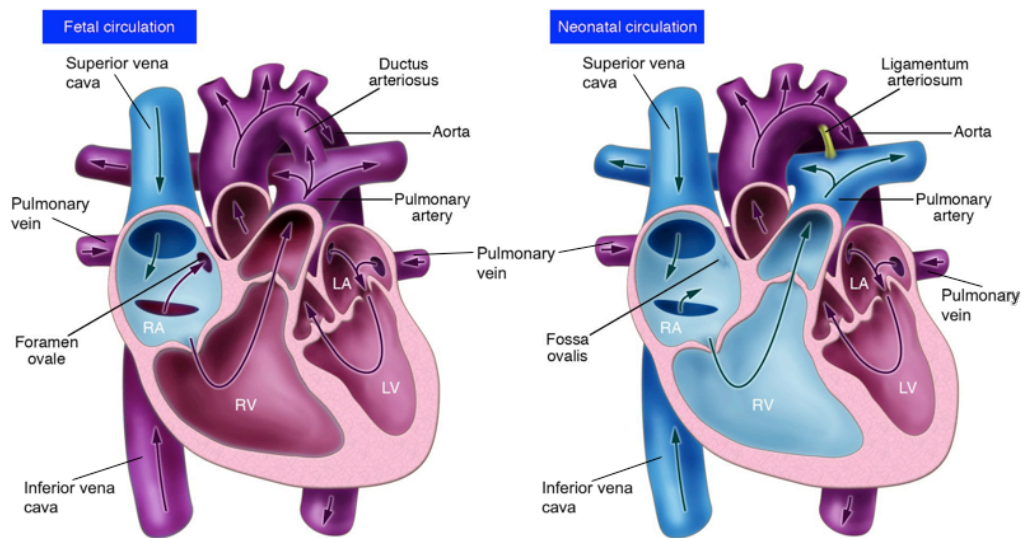


Figure 2.1: Schematic representation of the fetal circulation (left) with the foramen ovale and the ductus arteriosus which turn into the fossa ovalis and the ligamentum arteriosum in the neonatal circulation (right). Adapted from [11]

Continuous assessment of the CO during the transitional phase, where considerable changes occur in preload, contractility, pulmonary vascular resistance, systemic vascular resistance, and blood flow, can be useful since adaptation to these changes can be difficult. Preterm infants, especially the extremely preterm, are ill-prepared for the haemodynamic transition that occurs at birth, because of the structurally and functionally immature cardiovascular system. Their hearts have limited capacity to increase contractility and have less force during contraction, increasing the risk for low ventricular output and low systemic arterial pressure. [7, 8, 9]

Several other factors affecting cardiovascular function during the transitional period exist, for example perinatal asphyxia. The hypoxic insult in perinatal asphyxia leads to a decrease in SV and CO secondary to myocardial impairment and, in severe cases, can lead to cardiogenic shock. Another example is neonatal sepsis, which decreases the vasomotor tone and, if not compensated by an increase in CO, causes hypoperfusion and shock. Infants with intrauterine growth restriction show no change in left ventricle SV after birth and increase their HR to maintain CO, whereas healthy neonates show an increase in left ventricle SV and CO, and a decrease in HR. [11] Moreover, positive pressure ventilation can have a diminishing effect on the CO. A high mean airway pressure can cause overexpansion of the lung, which generates an increase in pulmonary vascular resistance and a decrease in pulmonary blood flow, resulting in a decrease in LVO. Additionally, high mean airway pressure increases intrathoracic pressure which reduces venous return. Therefore, continuous assessment of the CO, together with HR, arterial oxygen saturation, and blood pressure, can help with [9, 11]:

- Timely recognition and treatment of hypoperfusion, low flow, and early stages of shock, hence prevention of progressing to uncompensated shock leading to increased morbidity and mortality.
- Assessing the response to treatment.
- Establishing more knowledge about developmental cardiovascular physiology to improve treatment strategies.

2.3 Technological aspects of cardiac output monitoring

In adults, the gold standard for measuring the CO is the PA catheter using thermodilution. Due to size restraints, potential indicator toxicity, and the (vital) presence of extra- and intracardiac shunts in early life, this PA catheter, as well as other CO measurement methods, cannot be used in neonates. Other methods used to measure the CO in newborn infants include transcutaneous Doppler, MRI, transthoracic echocardiography (TTE), and electrical biosensing technologies.^[12]

The transcutaneous Doppler technique uses continuous wave Doppler to estimate and display blood flow across the aortic or pulmonary valve. It is fast and noninvasive, but the area of interest is not visualised. Moreover, the cross-sectional area of the outflow tract is estimated based on patient height, weight, and age, which can cause erroneous CO-values. When compared with transcutaneous Doppler, MRI has a better accuracy and repeatability, but because it is time-consuming, non-continuous, expensive, and not bedside available, it is unsuitable. TTE, however, is bedside available, noninvasive, and provides real-time information. Therefore, TTE is used most often to measure the CO in (preterm) neonates.^[8, 9, 12]

Another noninvasive, bedside available method to monitor the cardiac output is by using electrical biosensing technologies, such as transthoracic bioreactance (NICOM[®]), electrical cardiometry (ICON[®]), and whole-body bioimpedance (NICaS[®]). These technologies make it possible to continuously measure the cardiac output, but only few studies have investigated their application in (preterm) neonates.^[8, 9, 12]

2.3.1 Transthoracic echocardiography

TTE is a noninvasive method that is bedside available and provides real-time visualisation of the anatomical structures of interest based on the reflection of an ultrasound beam. Medical ultrasound systems use an acoustic signal with a frequency of 1-12 MHz which is sent into the patient with a transducer. The transducer consists of piezoelectric crystals. An electrical current causes these crystals to vibrate, generating an acoustic signal. When the signal hits tissue, part of the wave is reflected and scattered, while the other part passes through to underlying structures. The reflected signal, so called echo, makes its way back to the transducer where the sound waves induce the piezoelectric crystal to vibrate, converting the acoustic signal back into an electrical signal. The returned signal is processed to display an image of the anatomical structure in grey scale, where the brightness corresponds to the strength of the echo.^[13]

To show the velocity of a moving object, for example red blood cells in a vessel, Doppler imaging is used. There are two types of Doppler imaging, continuous wave Doppler and pulsed wave Doppler. In continuous wave Doppler, the signal and its echoes are continuously transmitted, received, and analysed, whereas in pulsed wave Doppler the sound waves are sent in short pulses with the echoes analysed in between. The major advantage of pulsed wave over continuous wave Doppler is that with pulsed wave Doppler the location of where to measure the velocity can be specified. By using the Doppler principle, the direction of the flow can be presented with a colour (colour Doppler).^[13]

In pulsed wave Doppler (Figure 2.2), the ultrasound signal is transmitted by one of the crystals (source crystal) and the echo that propagates back is recorded by another crystal (recording crystal). The sound wave returning to the transducer has been received and retransmitted by the moving object (red blood cell). The change of frequency between the transmitted signal (f_t) and the received signal (f_r) is called the Doppler shift or Doppler frequency (Δf). When the

Doppler shift is positive, the object is moving towards the transducer, which is shown in red using colour Doppler. An object moving away from the transducer generates a negative Doppler shift, shown in blue. The angle between the sound beam and the direction of the moving object, angle of insonation (θ), should be as small as possible. In other words, the ultrasound signal should be parallel to the direction of the moving object.^[13]

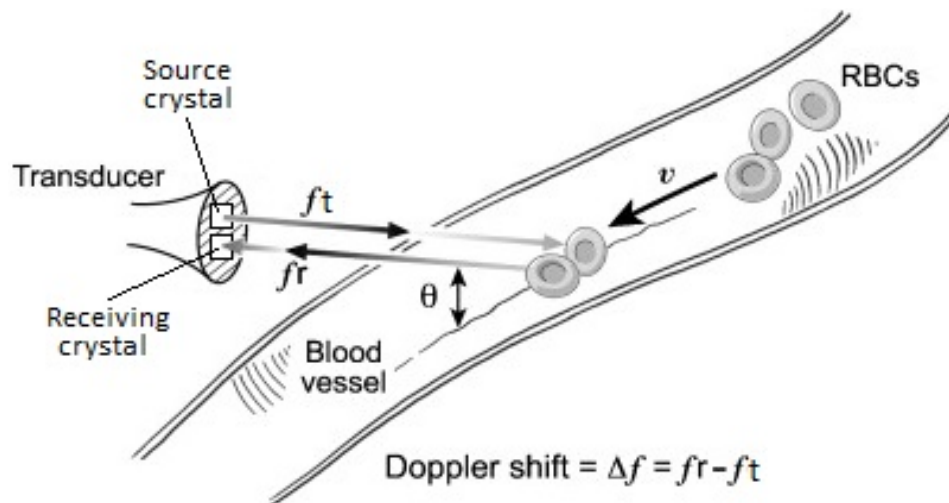


Figure 2.2: Schematic representation of pulsed-wave Doppler. With Δf : Doppler shift; f_t : frequency of transmitted signal; f_r : frequency of received signal; θ : angle of insonation; v : velocity and RBCs: red blood cells. Adapted from ^[2]

To determine the CO with TTE, both the diameter of the outflow tract and the velocity of the blood need to be determined. The diameter of the left ventricular outflow tract (LVOT) is measured in the parasternal long-axis view (Figure 2.3a) at the hinge points of the aortic valve (Figure 2.3b). For the right ventricular outflow tract (RVOT), the diameter is measured in the tilted parasternal long-axis view (Figure 2.4a) at the pulmonary valve insertion (Figure 2.4b). Both the diameter of the LVOT and the RVOT should be measured at end-systole. The measured diameters are then used to calculate the cross sectional area (CSA: $\pi \times (d/2)^2$) of the outflow tracts.^[3]

The velocity of the blood flow is recorded at the same site as where the diameter is measured. Using pulsed wave Doppler, the flow profile of the LVOT is measured in the apical five-chamber view or apical long-axis view (Figure 2.3c). For the RVOT, the parasternal long or short-axis view is used (Figure 2.4c). The Doppler frequency is used to plot the velocity over time (Figure 2.3d and 2.4d), from which the travelled distance of a column of blood during one heart cycle can be determined by calculating the area under the curve (velocity time integral – VTI). Because of the cardiopulmonary interaction, causing LVO to be highest at the end of expiration, VTI calculations should be averaged over three to five heart cycles to minimize the influence of respiration. Once the diameter and the VTI are obtained, the CO can be calculated with the following equation:

$$\text{CO [mL/min]} = \text{CSA [cm}^2\text{]} \times \text{VTI [cm]} \times \text{HR [beats/min]}. \quad (2.1)$$

In neonates this CO is normalized for bodyweight (mL/min/kg).^[3]

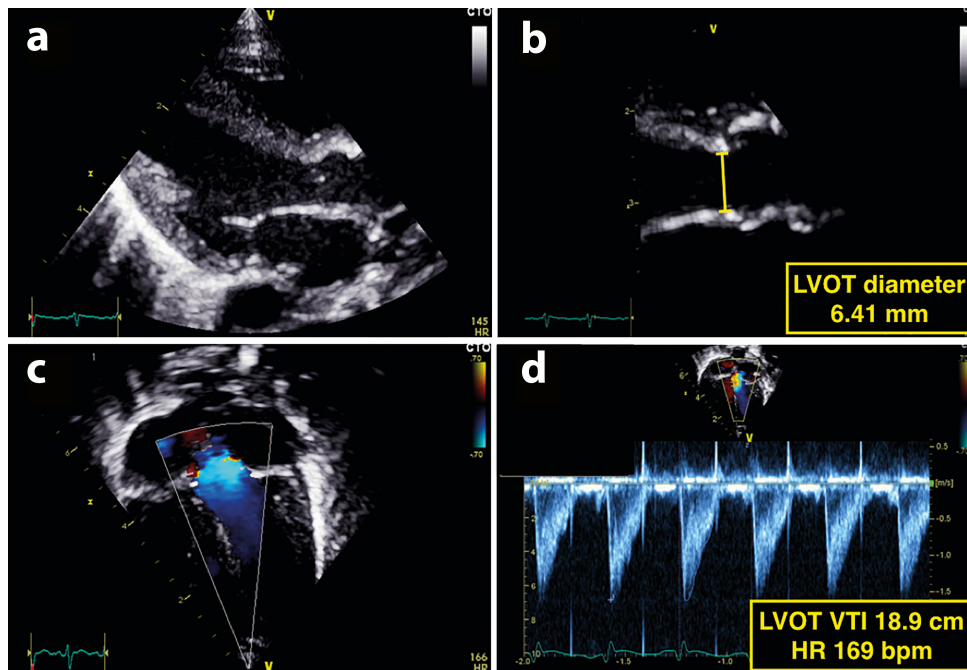


Figure 2.3: Example of LVO measurement with TTE. Reprinted with permission from [3]

De Waal et al. [14] investigated the diameter of the LVOT and RVOT in neonates of different weights. The median diameter of the LVOT was found to be 3.8 mm in neonates weighing less than 500 g and 5.7 mm in neonates with a weight between 1500-1750 g. For the RVOT, these values were 4.4 mm and 6.1 mm, respectively. [14] Normal CO values were reported to range from 150 to 350 mL/min/kg in (preterm) neonates without intracardiac (PFO) and extracardiac shunts (PDA). [3]

A literature review by Chew & Poelaert [15] of echocardiography CO measurements in paediatric patients showed that in all the studies reviewed the error percentage for echocardiography was around 30% when compared to thermodilution, dye dilution or the Fick method. This inaccuracy of echocardiography can be explained by looking at the disadvantages and limitations of echocardiography. First, if the diameter is incorrectly measured, this can cause a significant inaccuracy in CO, as the error in diameter is squared for the calculation of the CSA. Second, varying or incorrect probe position leads to a high intra- and interobserver variability. For example, an increase in the angle of insonation, which should be smaller than 20° , will underestimate the velocity of the blood flow. Third, the calculation of the CO assumes a perfect circle and laminar blood flow in the vessel. The velocity is measured at the centre of the vessel, where the flow is the highest, whereas the flow towards the vessel wall is slower. This causes overestimation of the CO. Other disadvantages of TTE are the requirement of specific training to perform CO measurements and that continuous measurements are not possible. [3, 15]

2.3.2 Electrical cardiometry

Osyka Medical's Noninvasive Cardiometer (ICON©) uses a method called electrical cardiometry (EC) to derive the CO. Four electrodes of 2.5 by 1.5 cm are placed on the patient's upper leg, thorax, neck, and head. The electrodes on the upper leg and head send a current of 2 mA with a frequency of 50 kHz into the thorax and especially into the aorta since blood is the most conducting tissue. [16] The resulting voltage, from which the conductivity is obtained, and an ECG are measured by the electrodes on the thorax and neck. [17, 18, 4]

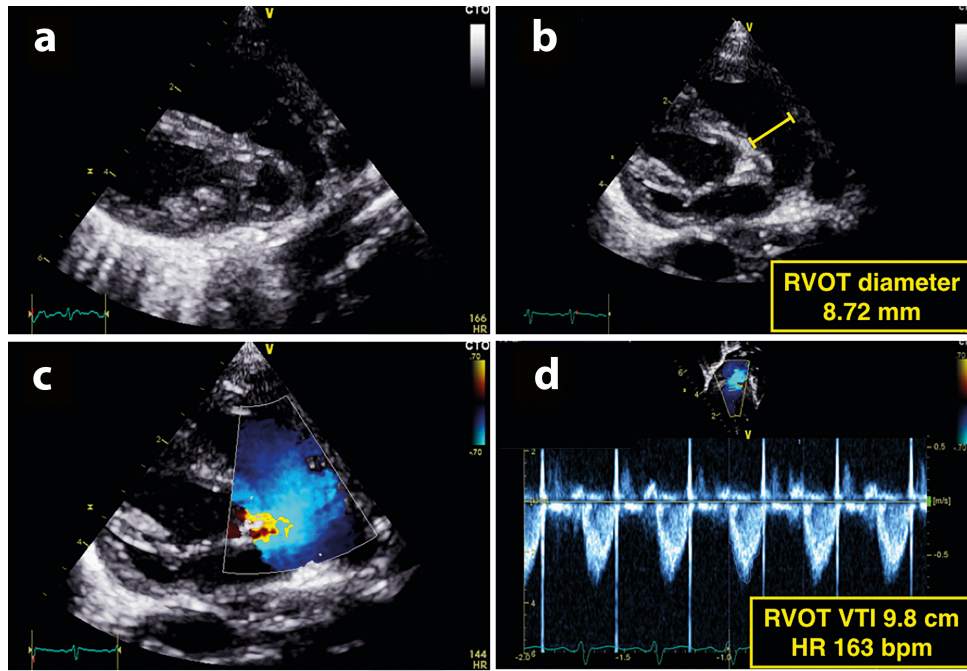


Figure 2.4: Example of RVO measurement with TTE. Reprinted with permission from [3]

During diastole, the electrical current meets more resistance (low conductivity) due to the random orientation of erythrocytes in the aorta. The pulsatile flow of systole forces the erythrocytes to align parallel to the blood flow and the electrical current, generating less resistance (high conductivity) of the electrical current. In Figure 2.5 the effect of the opening of the aortic valves on the impedance signal is shown. The shift from random orientation during diastole to the alignment of the erythrocytes at the onset of left ventricular ejection causes a sharp decrease of impedance, or in other words a sharp increase of conductivity. This abrupt decrease of impedance can be seen in Figure 2.5 as an increase in the inverted impedance signal ($-dZ(t)$). Below the inverted impedance signal the calculated time-derivative of $-dZ(t)$, $-\frac{dZ(t)}{dt}$, is shown, where its peak corresponds to the increase of conductivity. The height of the peak in $-\frac{dZ(t)}{dt}$ corresponds to the pace with which the erythrocytes align. Therefore, the higher the peak in $-\frac{dZ(t)}{dt}$, the higher the contractility of the heart and the aortic acceleration. [16, 18, 4, 19]

The peak aortic acceleration, that is $(\frac{dZ(t)}{dt})_{MIN}$, is used to approximate the mean blood velocity index \bar{v}_{FT} according to the following equation:

$$\bar{v}_{FT} = \sqrt{\frac{|(\frac{dZ(t)}{dt})_{MIN}|}{Z_0}}, \quad (2.2)$$

where Z_0 is the base impedance. Flow time correction (FT_C) is applied to adjust the left ventricular ejection time (LVET) for the heart rate, or R-R interval (T_{RR}), of the patient:

$$FT_C = \frac{LVET}{\sqrt{T_{RR}}}. \quad (2.3)$$

Equation 2.4 is then used to calculate the SV and CO (by multiplication with the HR), where V_{EPT} is the volume of electrically participating thoracic tissue derived from the weight and height of the patient. [16, 4, 19]

$$SV = V_{EPT} \times \bar{v}_{LVET} \times FT_C. \quad (2.4)$$

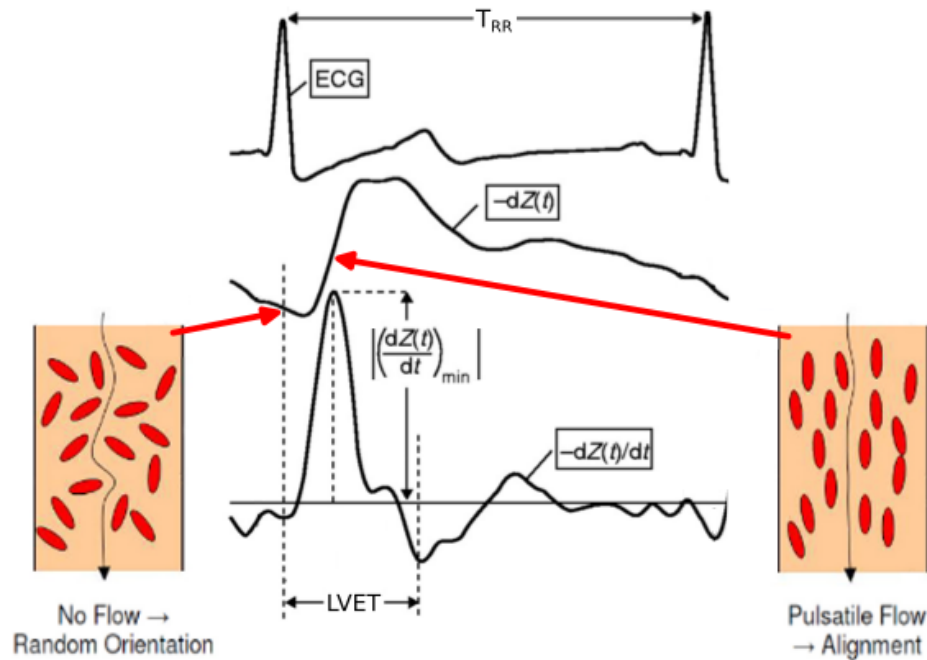


Figure 2.5: Explanatory figure of the EC theory. At the top, the ECG signal is shown. The inverted change of impedance (middle, $-dZ(t)$) increases upon opening of the aortic valve and decreases during diastole. The peak in the calculated time-derivative of $-dZ(t)$ (bottom, $-\frac{dZ(t)}{dt}$) corresponds to the peak aortic acceleration. LVET: left ventricular ejection time; T_{RR} : R-R interval. Adapted from [4]

Narula et al. [20] validated EC against the Fick principle in paediatric patients with congenital structural heart disease and found a percent bias and error of 0.1% and 11.6%, respectively. Other validation studies in (preterm) neonates and children used TTE as reference method and reported the percent bias to range between 0.7 and 8.6% and percent error ranging from 19.7 to 60.2% (Table 2.1). [21, 22, 23, 24, 25] Moreover, EC was found to detect the haemodynamic response to bradycardia and/or desaturation [26], but has limitations in detecting CO during high-frequency ventilation. [24]

Besides measuring HR, SV, and CO, the cardiometer also gives an indication for the signal quality (signal quality index – SQI) and estimates parameters of the vascular system, contractility, fluid status, and oxygen status. For example, it can estimate the (variation of) index of contractility, thoracic fluid content, stroke volume variation, and the systemic vascular resistance based on the input of mean arterial pressure and central venous pressure. The SQI given by EC is a measure of the validity of the prior ten data points (heart cycles) expressed as a percentage. A classified algorithm is used to determine the validity of a data point based on both the ECG and impedance signal. If one of the last ten data points is invalid, the SQI drops by 10%. [17]

Table 2.1: Validation studies of EC. NA: not available.

Reference	Subjects	Comparison	CO _{mean}	Mean Bias	LOA	Bias%	Error%
Noori, 2012 [21]	20 term neonates, mean gestational age 39.2 ± 1.1 weeks, mean weight 3094 ± 338 g	EC vs TTE (LVO)	538 mL/min	-4 mL/min	-238 – +229 mL/min	-0.7%	43.6%
Rauch, 2013 [22]	64 obese children and adolescents, median age 12.52 years (7.9 – 17.6 years), median weight 78 kg (38 – 155 kg)	EC vs TTE	5.28 L/min	0.15 L/min	-0.91 – +1.21 L/min	2.8%	19.7%
Grollmuss, 2014 [23]	28 premature neonates, mean gestational age 31.7 ± 3.1 weeks, mean weight 1618 ± 346 g	EC vs TTE	265.3 mL/kg/min	8.9 mL/kg/min	-53.8 – +71.6 mL/kg/min	3.4%	24%
Song, 2014 [24]	40 preterm neonates, mean gestational age 27 weeks (23 – 31 weeks), mean weight 1072 g (530 – 1596 g)	EC vs TTE (LVO)	218 mL/kg/min	-18.8 mL/kg/min	-151.6 – +113.8 mL/kg/min	8.6%	60.2%
Boet, 2016 [25]	79 preterm neonates, mean gestational age 31 ± 3.2 weeks, mean weight 1440 ± 533 g	EC vs TTE (LVO)	NA	-0.21 L/min	-0.55 – +0.15 L/min	NA	NA
Narula, 2017 [20]	50 paediatric patients with congenital structural heart disease, mean age 6.4 ± 4.8 years	EC vs pulmonary artery catheterization Fick principle	4.22 L/min/m ²	0.0051 L/min/m ²	±0.49 L/min/m ²	0.1%	11.6%

3 AIM

The main goal of this study is to determine the accuracy, reliability, and applicability of EC to measure CO in critically ill newborns. As a new CO monitoring device, EC ideally meets several requirements for its application in neonates. First and foremost, it must be validated against a gold standard reference technology. Since the gold standard for CO measurements cannot be used in neonates, as explained in section 2.3, TTE is often used as a reference method in existing literature. Second, the device should be accurate along the range of gestational age and birth weight, and in neonates with a PDA and/or PFO. Third, it is required to provide continuous measurements and the CO values must be recordable along with the other haemodynamic parameters. Finally, the device should be reliable, practical, noninvasive, and easy to apply and interpret.^[27]

Based on the system requirements, the following components will be investigated:

- Validation of EC SV and CO values with reference method TTE.
- Ability of EC to monitor the trend of the CO.
- Comparison between the HR measured by EC and the HR measured with the ECG electrodes (reference).
- Influence of patient weight and height on EC CO.
- Influence of TTE on EC SQI, SV and CO, and patient parameters HR and SpO₂.
- Usability.

4 METHODS

4.1 Population and study design

To determine the accuracy, reliability, and applicability of EC, an observational cohort study was performed. Patients admitted to the NICU of the Radboudumc Nijmegen, the Netherlands, with a gestational age between 26 and 42 weeks were eligible for inclusion. Primary exclusion criteria for this study were clinical instability, congenital heart defects, skin conditions, high frequency ventilation, and severe oedema. Additionally, patients were excluded from the study in the case of a language barrier in communication with the parents.

4.2 Data acquisition

After inclusion, the patients were connected to the cardiometer according to the instructions from the manufacturer. First, the electrodes were placed inside the incubator for at least five minutes to warm the conductive gel to improve signal quality. Patients' weight and height were measured and entered in the cardiometer together with the postnatal age. The electrodes were placed according to the positions depicted in Figure 4.1. The first electrode (A) was positioned on the right temporal area. If this area was unavailable, for example because of the patient's hair, the electrode was relocated to the forehead. The other electrodes were placed on the right side of the neck above the clavícula and near the carotid artery (B), on the left midaxillary line of the thorax at the vertical level of the xiphoid (C), and on the left inner thigh (D).

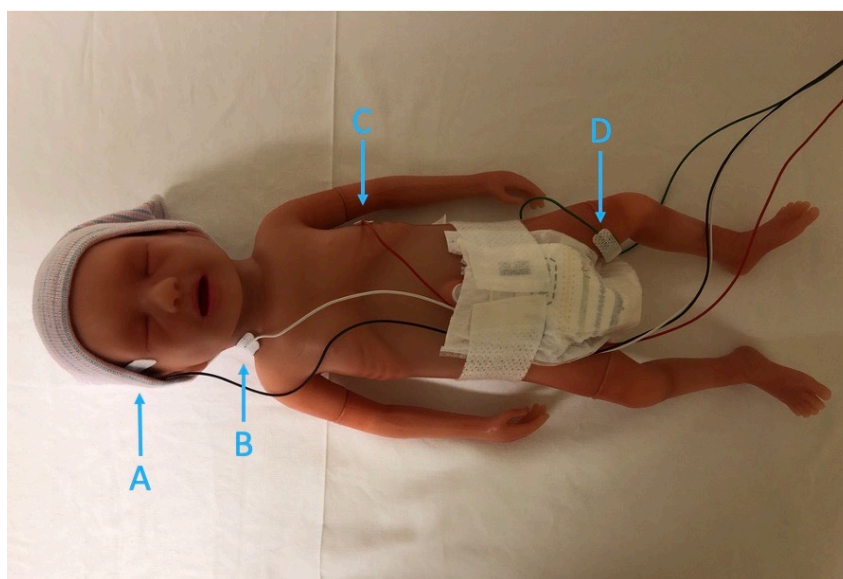


Figure 4.1: Representation of the electrode positions on a (premature) baby mannequin. A: right temporal area; B: right side of the neck; C: left midaxillary line at xiphoid level; D: left inner thigh.

The HR, SV, and CO were continuously measured with EC (HR_{EC} , SV_{EC} , CO_{EC}) for as long as the electrodes remained adhered and in position, or until the SQI became low (below 70%) or the patient was discharged from the NICU. HR_{EC} , SV_{EC} , and CO_{EC} were collected beat-to-beat and displayed on the Philips IntelliVue monitor using the IntelliBridge EC10. Due to the limited data storage capacity of the cardiometer, the recording period was set to one minute. That is, the last known beat-to-beat value of the EC parameters at the time of recording was saved on the device. The EC data (except for HR_{EC}) was also stored in the Philips Data Warehouse, along with the recorded physiological parameters of the patient, such as the arterial oxygen saturation and the respiratory rate. During the measurement, patient events such as the beginning and end of nursing and TTE were registered as an event on the Philips IntelliVue monitor and stored in the Philips Data Warehouse.

For the validation of EC, TTE was performed by a skilled neonatologist when the patient was connected to the cardiometer. To limit additional disturbance of the patient by TTE, no specific time windows were used. The aim was to perform TTE at least once per day. To calculate the CSA, the diameter of the outflow tract was measured once per TTE measurement at the hinge points of the aortic valve (LVOT) and at the pulmonary valve insertion (RVOT) at end-systole. The diameters of each TTE measurement in a single patient were averaged to minimise the influence of erroneous diameter measurements on the CO, assuming the diameter did not change within the short time between TTEs. For the velocity of the blood flow, three blood flow profile recordings were obtained within the LVOT and RVOT. Per recording the VTI calculations were averaged over three to five different heart cycles. The left and right ventricular stroke volume (LVSV, RVSV) were determined by multiplication of the CSA and VTI of the LVOT and RVOT ($LVSV_{TTE}$, $RVSV_{TTE}$). The LVO and RVO were calculated using equation 2.1 (LVO_{TTE} , RVO_{TTE}).

To be able to judge the usability of EC, attention was paid to several aspects during the measurements. For example, durability of the electrodes, calibration time, user interface, and ability to record the data along with other haemodynamic parameters.

4.3 Data analysis

The acquired data of the HR, SpO_2 , EC (CO, SV, SQI), and patient events were retrieved from the Philips Data Warehouse and analysed using MathWorks' MATLAB, version 2019b.

4.3.1 Validation of electrical cardiometry

For the validation of EC with reference method TTE, epochs within the CO_{EC} and SV_{EC} data were identified for the time during which TTE was performed simultaneously. To create these epochs, the timestamps of the registered patient events were used. The obtained epochs were then filtered in two steps. First, data points with a SQI below 70% were removed from the epochs, as the manufacturer advises to rely only on data with a SQI of 70% or higher. Second, the data points with a value above or below the epoch's mean plus/minus two times the standard deviation (SD) were considered outliers and discarded. The average and SD of the resulting EC data was calculated and used for validation and trend analysis.

Validation between EC and TTE was assessed by analysis of the agreement and correspondence in categorisation between the two methods. The agreement between CO_{EC} and LVO_{TTE} or RVO_{TTE} was determined by Bland-Altman analysis. With this analysis, the mean difference (bias) and SD of the bias were obtained. Limits of agreement (LOA), bias percentage (bias%)

and error percentage (error%) were calculated according to equation 4.1, 4.2, and 4.3, respectively. The LOA and error% were based on a 95%CI, hence the 1.96SD.

$$\text{LOA} = \text{mean bias} \pm 1.96 \times \text{SD} \quad (4.1)$$

$$\text{bias\%} = \frac{\text{mean bias}}{\text{CO}_{\text{TTE}}} \times \quad (4.2)$$

$$\text{error\%}_{\text{EC+TTE}} = \frac{1.96 \times \text{SD}_{\text{bias}}}{\text{mean CO}_{\text{TTE}}} \times 100\% \quad (4.3)$$

According to Critchley & Critchley [28] the error% should be less than 30% for good agreement and to accept the new method, assuming a reference method with an error% of 20. Since TTE is known to have an error% of 30, the precision of EC can be underestimated. Therefore, the acceptable error% needs to be adjusted for the 30% error of TTE, resulting in a combined error%_{EC+TTE} of 42.4%. [29] Another option is to correct for the error% of TTE when calculating the specific error% of EC:

$$\text{error\%}_{\text{EC}} = \sqrt{\text{error\%}_{\text{EC+TTE}}^2 - \text{error\%}_{\text{TTE}}^2} \quad (4.4)$$

Similar calculations were performed to determine the agreement between SV_{EC} and LVSV_{TTE}/RVSV_{TTE}.

Because the main interest of the clinician is to know whether the patient is in a low, normal, or high CO state, and it is of less interest to know the absolute value, CO_{EC}, LVO_{TTE}, and RVO_{TTE} values were categorised per state. In this study, a CO below 150 mL/min/kg was considered as low, 150-350 mL/min/kg as normal, and above 350 mL/min/kg as high. To demonstrate if the CO values of the two methods were categorised similarly, a scatter plot was created in which the areas of low, normal, and high CO were marked. Furthermore, the percentage of similarly categorised data was calculated, as well as the percentage of the data where CO_{EC} was in a lower or higher category than LVO_{TTE} or RVO_{TTE}.

4.3.2 Trending ability of electrical cardiometry

To assess the ability of EC to track changes in CO, concordance and polar plot analysis were performed. A 4-quadrant concordance plot was created, which was used to analyse the direction of change in CO. The difference in CO between two consecutive epochs in a patient was calculated and $\Delta\text{CO}_{\text{EC}}$ was plotted against $\Delta\text{LVO}_{\text{TTE}}$ or $\Delta\text{RVO}_{\text{TTE}}$. Concordance rate was determined by the number of data points in quadrant one (upper right) and three (lower left) of the concordance plot divided by the total amount of data points. An exclusion zone of 15% of mean CO, as proposed by Critchley et al. [30], was applied to eliminate small changes in CO as these were considered as clinically irrelevant and thus random noise. A concordance rate >95% is considered as good trending, >90% acceptable, and <90% poor.

Concordance analysis has a few limitations. Since the length of the X-Y vector in the concordance plot is the hypotenuse of the change in COTTE and CO_{EC} ($\sqrt{\Delta\text{COTTE}^2 + \Delta\text{CO}_{\text{EC}}^2}$), bias can be created if either ΔCOTTE or $\Delta\text{CO}_{\text{EC}}$ is significantly bigger than the other, because the larger value determines the overall length of the vector. Moreover, there is considered to be concordance if the point lies within 45° from the line of identity (Y = X), but this ignores the degree of agreement between the two methods. Because of these limitations, polar plot analysis was performed as well.

For the generation of the polar plot the Cartesian data of the concordance plot was converted to polar coordinates according to the method proposed by Critchley et al. [31] From the polar

plot the angular bias with radial LOA (95% confidence interval) were determined. Instead of the hypotenuse, the polar plot uses the mean value of ΔCOTTE and $\Delta\text{CO}_{\text{EC}}$ (radius). Agreement between the two methods is shown by the angle the vector makes with the horizontal (0°) axis. The exclusion zone was scaled down to 10%, corresponding to a 1.5 scaling factor based on the transformation from the Cartesian hypotenuse to the polar radius. Good trending is assumed when the angular bias is smaller than $\pm 5^\circ$ and the radial limits of agreement are $< \pm 30^\circ$. [30]

4.3.3 Heart rate comparison

To verify whether the HR_{EC} compares to the HR from the ECG (HR_{ECG}), the covariance and agreement between the two methods were determined. Because HR_{EC} was recorded once per minute on the cardiometer, the samples closest to the timestamps from HR_{EC} were retrieved from the beat-to-beat HR_{ECG} data. Per patient a time interval of four hours was selected from the first 24 hours of the measurement. Interval selection was based on the highest ratio of data with a SQI of 100%, which was calculated using a moving time window. The cross-covariance between the HR_{EC} and HR_{ECG} data from the resulting interval per patient was computed, giving the correlation and time lag between the two data sets. Furthermore, the mean, SD, and coefficient of variation (COV) of HR_{EC} and HR_{ECG} during the interval were calculated, and Bland-Altman analysis was performed to determine the agreement.

4.3.4 Influence of patient weight and height

The influence of patient weight and height on CO_{EC} was assessed by calculating the correlation coefficient between CO_{EC} , LVO_{TTE} or RVO_{TTE} and weight or height. For CO_{EC} , the average CO_{EC} value of the period during which TTE was performed, as explained in section 4.3.1, was used. Patient weight and height measured at the start of EC measurement were used for the calculation of the correlation with all CO measurements in a single patient. For example, if a total of four TTE's were performed in one patient, the patient's weight and height from the first day of EC measurement was used for all four measurements. Since the weight can be entered in the electrical cardiometer with an accuracy of 50 g and the height with an accuracy of 0.5 cm, the weight and height used for the calculation of correlation with CO_{EC} were rounded to the nearest value.

4.3.5 Influence of transthoracic echocardiography

To determine the influence of TTE on EC SQI, SV and CO, and patient parameters HR and SpO_2 , the data was split into three separate intervals: one hour before the beginning of TTE (1), the duration of TTE (2), and one hour after the end of TTE (3), see Figure 4.2. SV and CO data points with a SQI below 70% were removed from the intervals and the percentage of data with a SQI below 70% was calculated. For each haemodynamic parameter – SV, CO, HR, and SpO_2 – the mean and SD of the three intervals combined were determined to create a filter to remove outliers (mean \pm 2SD). The parameters' maximal and minimal values were determined for every interval, after which the outlier filter was applied and the mean, COV, and percentage of outliers were calculated per interval. IBM SPSS Statistics, version 27, was used to determine whether there was a significant difference between the three intervals. This was done for each parameter and its statistics, i.e. the mean, COV, maximal and minimal value, and the percentage of outliers. Since not all data was normally distributed, Friedman's ANOVA was applied to the paired data. Kendall's W was computed to demonstrate the effect size, where a value of 0.1 is interpreted as a small effect, 0.3 as a moderate effect, and 0.5 as a large effect. [32] When there was a statistically significant difference ($p < 0.05$), post hoc tests were performed using the Wilcoxon signed-rank test with Bonferroni correction ($p < 0.017$) to establish between which specific intervals the differences were present.

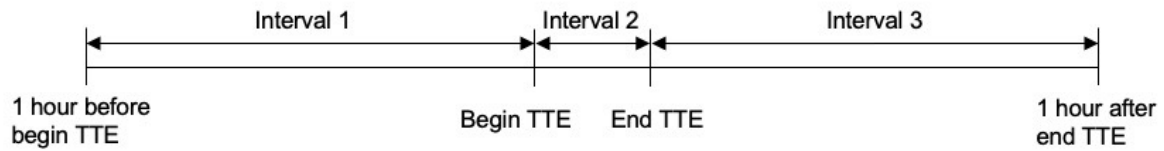


Figure 4.2: Timeline of the intervals used to determine the influence of TTE on the haemodynamic parameters and SQI.

4.3.6 Usability: durability of electrodes

For the assessment of the durability of the electrodes, the proportion of samples with a good SQI ($\geq 70\%$) was calculated per hour for the entire EC measurement period. Overall mean and trend of the SQI were calculated as well. The resulting data was plotted for each subject individually.

5 RESULTS

5.1 Population

During a period of five months, 19 patients were included of whom 10 were male (Table 5.1). 43 paired EC and TTE measurements were performed, mostly within the first 72 hours after the start of the EC measurement, with an average of two paired measurements per patient (range 1 – 4). In two cases it was impossible to determine the RVO due to turbulence in the PA caused by a PDA with left-to-right shunt. The measurements with EC had a median duration of 78 hours (IQR 65.5 – 109), with a minimum of 6 hours and a maximum 213 hours. Of the included patients, 12 patients were supported by nasal continuous positive airway pressure (nCPAP), 2 by low flow oxygen, and 5 patients did not receive any ventilatory support.

5.2 Validation of electrical cardiometry

The overall means \pm SD of CO_{EC} , LVO_{TTE} , and RVO_{TTE} during the TTE epochs were 224 ± 40 , 244 ± 98 , and 335 ± 112 mL/min/kg, respectively. Bland-Altman analysis of CO_{EC} and LVO_{TTE} , as shown in Figure 5.1, gave a mean bias of -19.6 mL/min/kg with LOA of 192.4 and -231.6 mL/min/kg. The bias% was found to be -8% and the uncorrected error% (error% $_{EC+TTE}$) was 86.9%. When corrected for the error% of TTE, the error% of EC was established at 81.6%. As shown in Figure 5.2, the mean bias between CO_{EC} and RVO_{TTE} was -110.3 mL/min/kg with an upper and lower LOA of 102.2 and -322.8 mL/min/kg, respectively. The bias% was -32.9% and the corrected error% was 55.9% (uncorrected 63.4%). It is apparent from both Figure 5.1 and Figure 5.2 that there is a significant ($p < 0.001$), negative correlation between the difference and the mean of CO_{EC} and LVO_{TTE} or RVO_{TTE} . This indicates that for the RVO_{TTE} , bias between CO_{EC} and RVO_{TTE} enlarges with increasing CO, whereas bias between CO_{EC} and LVO_{TTE} enlarges with decreasing CO before the regression line intersects zero bias and after this point bias enlarges with increasing CO. In other words, CO_{EC} overestimates LVO_{TTE} before the intersection and underestimates it after the intersection.

Table 5.1: Patient demographics (N=19).

	Median	IQR	Range
Postmenstrual age at start EC measurement (weeks + days)	29+3	28+1 – 31+0	27+5 – 32+5
Postnatal age (days)	6	5 – 13	1 – 26
Weight (g)	1109	983.5 – 1380	880 – 2110
Height (cm)	36.5	34 – 39	31 – 44.5
Gestational age at birth (weeks + days)	28+0	27+0 – 29+4	26+0 – 32+4
Birthweight (g)	1050	900 – 1370.5	745 – 2176

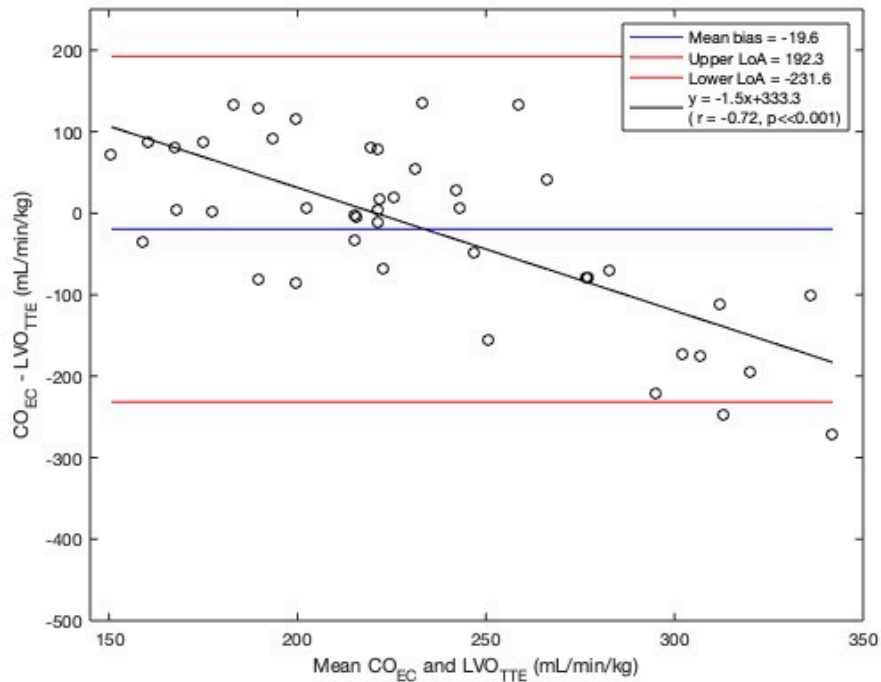


Figure 5.1: Bland-Altman analysis of CO_{EC} and LVO_{TTE} (N = 43).

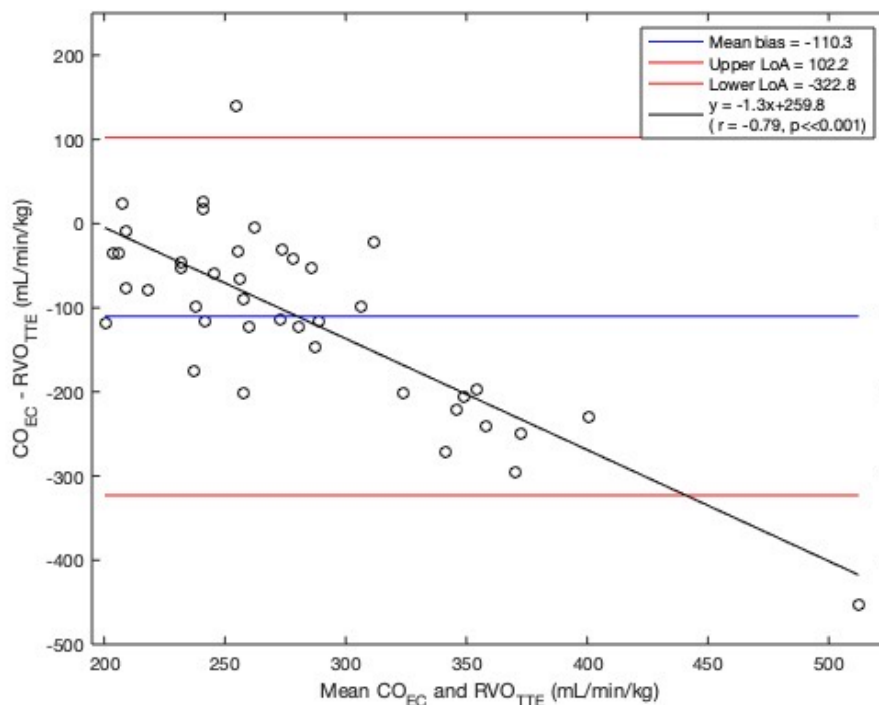


Figure 5.2: Bland-Altman analysis of CO_{EC} and RVO_{TTE} (N = 41).

For the SV, the overall means \pm SD of SV_{EC} , LVS_{TTE} , and RVS_{TTE} during the TTE epochs were 1.4 ± 0.3 , 1.5 ± 0.5 , and 2.1 ± 0.7 mL/kg, respectively. There was a mean bias of -0.1 mL/kg (6.0% bias%) between SV_{EC} and LVS_{TTE} with LOA of 1.2 and -1.3 mL/kg, resulting in an error% of 85.1. For the RVS_{TTE} , the mean bias was -0.7 mL/min (33.8% bias%) with LOA of 0.6 and -2.0 mL/min (61.6% error%). Visual representation of these Bland-Altman analyses can be found in the Appendix 8 Figure 1 (LVS) and 2 (RVS).

The scatter plots shown in Figure 5.3 and 5.4 depict the relation between CO_{EC} and LVO_{TTE} , and CO_{EC} and RVO_{TTE} , respectively. In these figures, regions of low, normal, and high CO are displayed in respective blue, green, and red. The values of CO_{EC} and LVO_{TTE} were similarly categorised in 58.1% of the paired measurements. Of the remaining data, CO_{EC} values were classified in a lower category than LVO_{TTE} in 23.3% and in a higher category in 18.6% of the cases. For the comparison with RVO_{TTE} , the categorisation was similar in 63.4% and in the remaining 36.6% CO_{EC} was classified in a lower category.

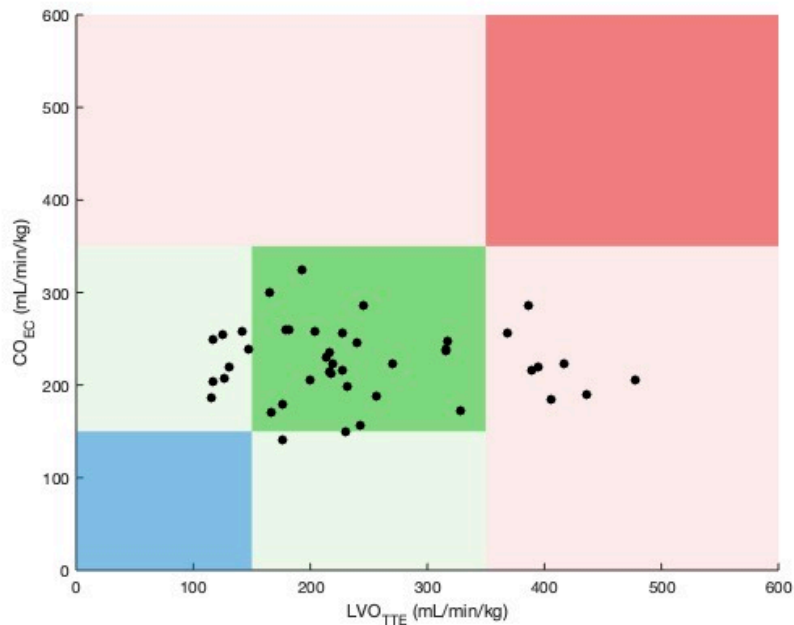


Figure 5.3: Scatter plot of CO_{EC} and LVO_{TTE} with marked regions for categorisation (N = 43). Blue: low CO (<150 mL/min/kg); green: normal CO (150-350 mL/min/kg); red: high CO (>350 mL/min/kg).

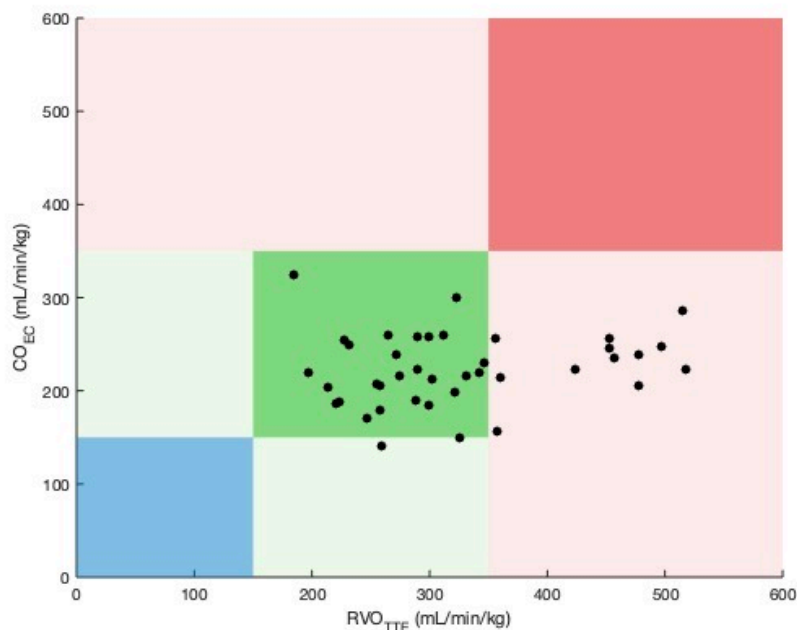


Figure 5.4: Scatter plot of CO_{EC} and RVO_{TTE} with marked regions for categorisation (N = 41). Blue: low CO (<150 mL/min/kg); green: normal CO (150-350 mL/min/kg); red: high CO (>350 mL/min/kg).

5.3 Trending ability of electrical cardiometry

For the concordance and polar plot analysis, 24 LVO and 22 RVO data points giving the difference between two consecutive measurements were available. In Figure 5.5 the concordance plot of $\Delta\text{CO}_{\text{EC}}$ and $\Delta\text{LVO}_{\text{TTE}}$ is shown with a concordance rate of 55.5%. The exclusion zone was set at 30 mL/min/kg which was approximately 15% of the mean CO. Figure 5.6 shows the concordance of $\Delta\text{CO}_{\text{EC}}$ and $\Delta\text{RVO}_{\text{TTE}}$ with a concordance rate of 50%. Both concordance rates suggest poor trending as these are below the 90% lower limit for acceptable trending. Furthermore, closer inspection of the results depicted in Figure 5.5 and 5.6 shows that the range $\Delta\text{LVO}_{\text{TTE}}$ and $\Delta\text{RVO}_{\text{TTE}}$ is rather large (-150 to 50 mL/min/kg), whereas $\Delta\text{CO}_{\text{EC}}$ has a smaller range of -50 to 50 mL/min/kg.

The polar plots of CO_{EC} and LVO_{TTE} , and CO_{EC} and RVO_{TTE} are presented in Figure 5.7 and 5.8, respectively. The exclusion zone was set at 20 mL/min/kg, approximating the 10% mean CO and 1.5 times smaller than the exclusion zone used for the concordance analysis. For the polar plot analysis of LVO the angular bias was found to be -29.5° (330.5°) with radial LOA of $\pm 60^\circ$. Analysis of RVO gave an angular bias of -23.6° (336.4°) with radial LOA of $\pm 60^\circ$. Analysis of EC for both LVO and RVO indicate poor trending ability as the angular bias and radial LOA are larger than the respective $\pm 5^\circ$ and $\pm 30^\circ$ limits for good trending.

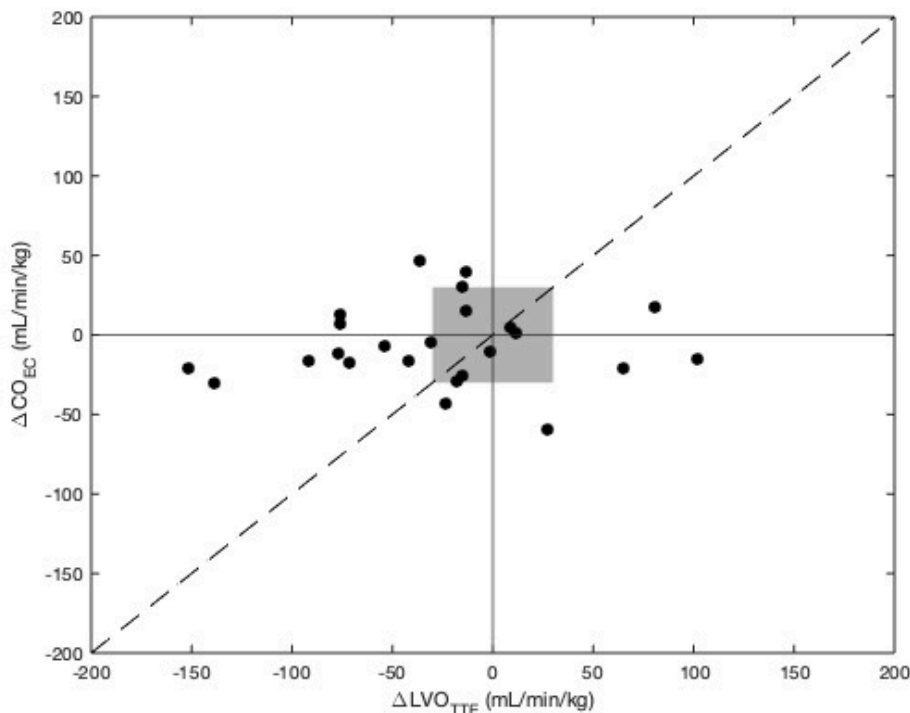


Figure 5.5: Concordance plot of CO_{EC} and LVO_{TTE} with an exclusion zone (in grey) of 30 mL/min/kg (N = 24). The dashed line represents the angle of identity.

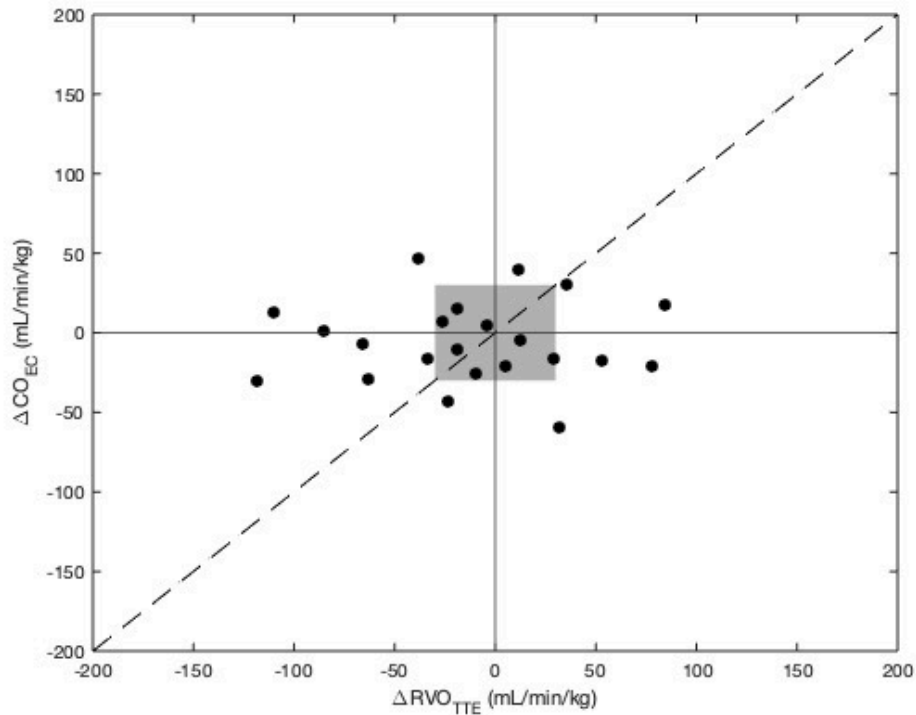


Figure 5.6: Concordance plot of CO_{EC} and RVO_{TTE} with an exclusion zone (in grey) of 30 mL/min/kg ($N = 22$). The dashed line represents the angle of identity.

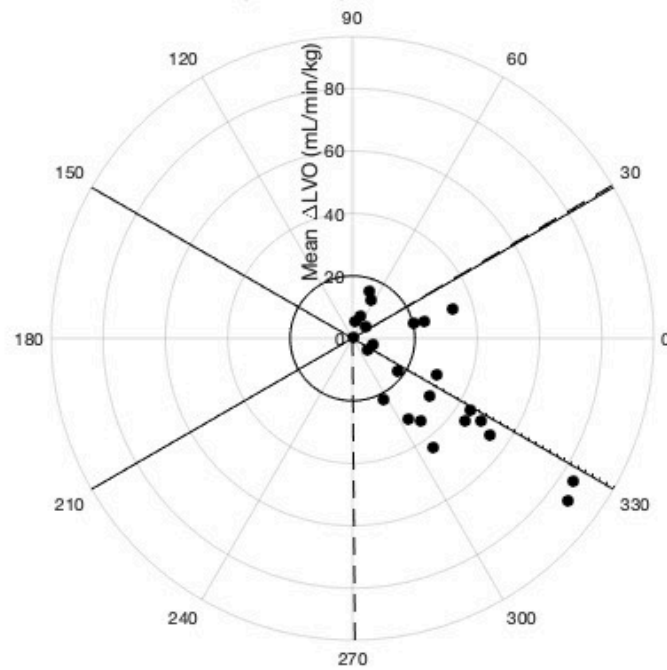


Figure 5.7: Polar plot of CO_{EC} and LVO_{TTE} with an exclusion zone of 20 mL/min/kg ($N = 24$). The dotted line represents the angular bias (-29.5°) and the dashed lines represent the radial limits of agreement (30.5° & -89.5°).

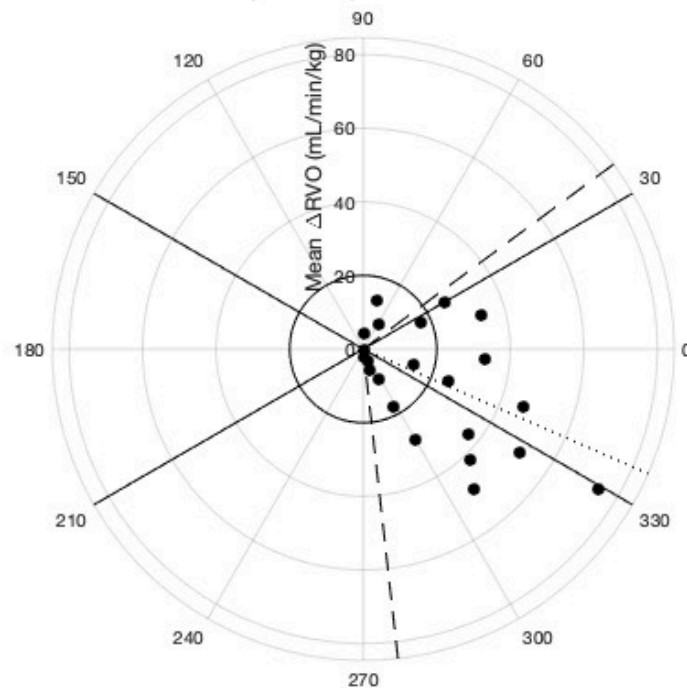


Figure 5.8: Polar plot of CO_{EC} and RVO_{TTE} with an exclusion zone of 20 mL/min/kg (N = 22). The dotted line represents the angular bias (-23.6°) and the dashed lines represent the radial limits of agreement (36.4° & -83.6°).

5.4 Heart rate comparison

The overall means \pm SD (COV) of HR_{EC} and HR_{ECG} during the four-hour interval were 157.5 ± 12.6 (5.5%) and 157.6 ± 12.5 (5.9%) beats/min, respectively. The summarised results obtained from the cross-covariance between HR_{EC} and HR_{ECG} of all subjects gave a mean \pm SD covariance of 0.60 ± 0.18 with a range of 0.29 to 0.90. There was an average time lag between HR_{EC} and HR_{ECG} of 1 minute (range 0 - 6), where HR_{EC} was ahead of HR_{ECG} . In Figure 5.9 the cross-covariance of a single patient is shown as an example, where the peak shows that a covariance of 0.782 was found at a time lag of 1 minute. HR_{EC} and HR_{ECG} of this patient in the four-hour interval are presented in Figure 5.10, along with the SQI. The top part of the figure shows the original data. In the bottom graph, HR_{ECG} data is shifted for the one-minute time lag. It can be seen that HR_{EC} has a similar trace as HR_{ECG} . Also, when there was a sudden drop in HR there was also a drop in SQI. Figure 5.11 shows the difference between HR_{EC} and HR_{ECG} over time, again with the original data at the top and the shifted data at the bottom. This figure illustrates that when the HR_{ECG} is shifted for the time lag, the difference between the two methods is negligible.

The summarised results of the Bland-Altman analysis gave a mean bias of -0.12 beats/min with a SD of the bias of 9.5 beats/min. The bias% was found to be -0.04% and the error% was 5.9%. For the shifted HR_{ECG} data, this resulted in a mean bias of -0.011 beats/min, a SD of the bias of 8.3 beats/min, and bias% and error% of -0.002% and 5.2%, respectively. In Table 1 and 2 of Appendix 8 the mean, SD, and the range of the results from the Bland-Altman analysis of the original and shifted HR data of all patients are shown. These results indicate a good agreement between HR_{EC} and HR_{ECG} .

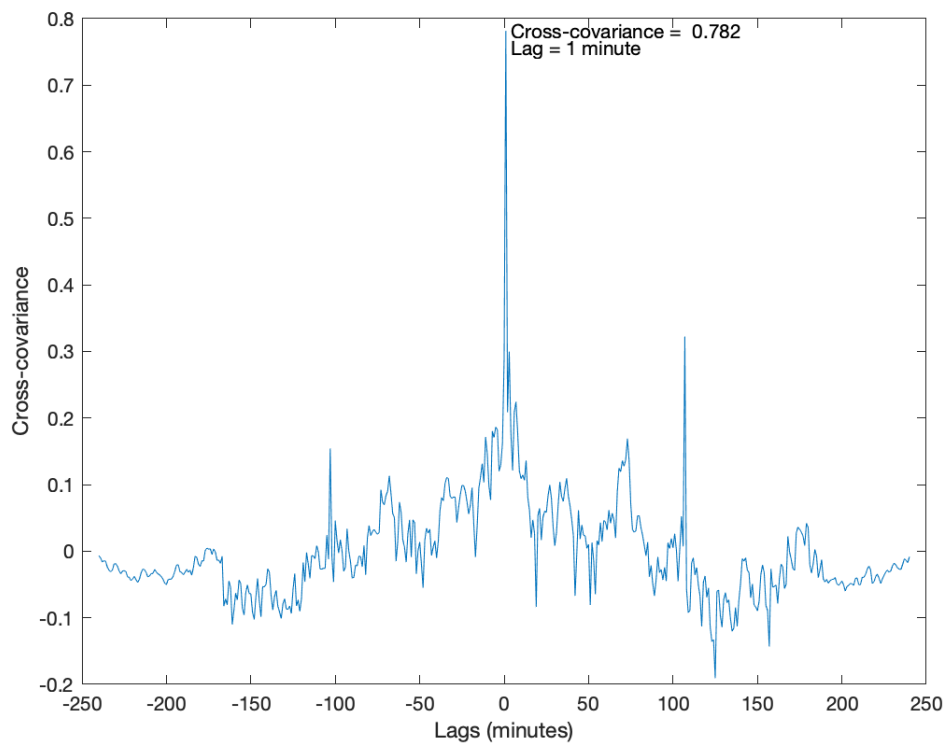


Figure 5.9: The cross-covariance between HR_{EC} and reference method HR_{ECG}.

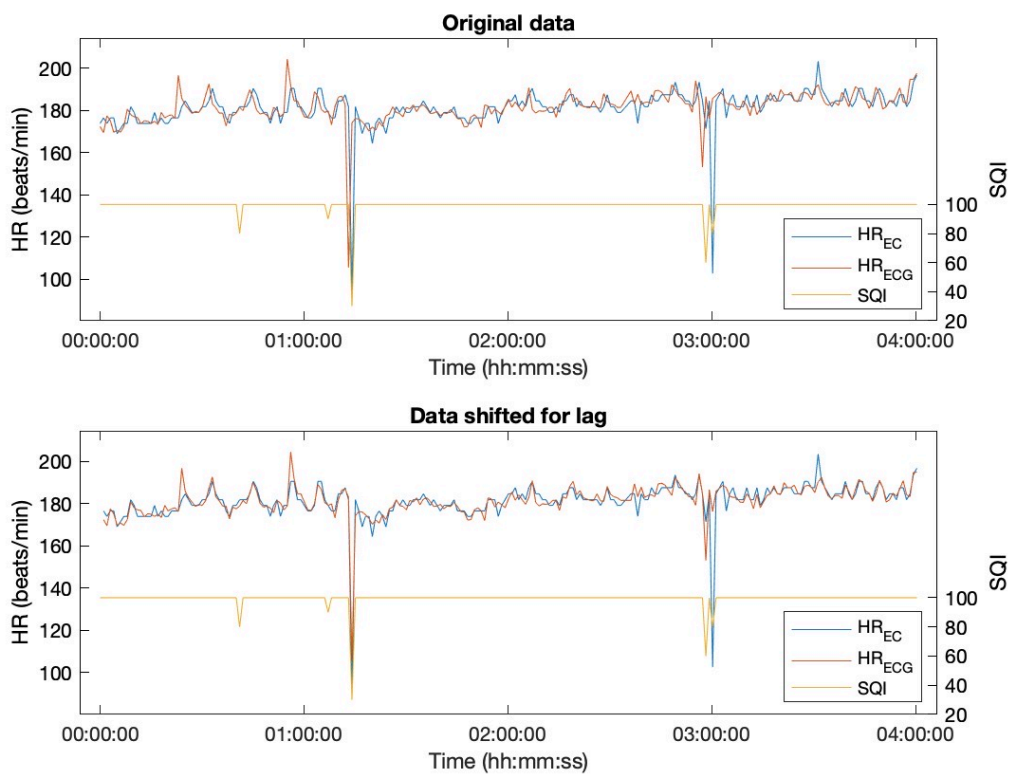


Figure 5.10: HR data of a single patient over time along with the SQI. At the top, the original HR_{EC} and HR_{ECG} is shown. At the bottom, the HR_{ECG} data is shifted forward for the obtained lag of 1 minute.

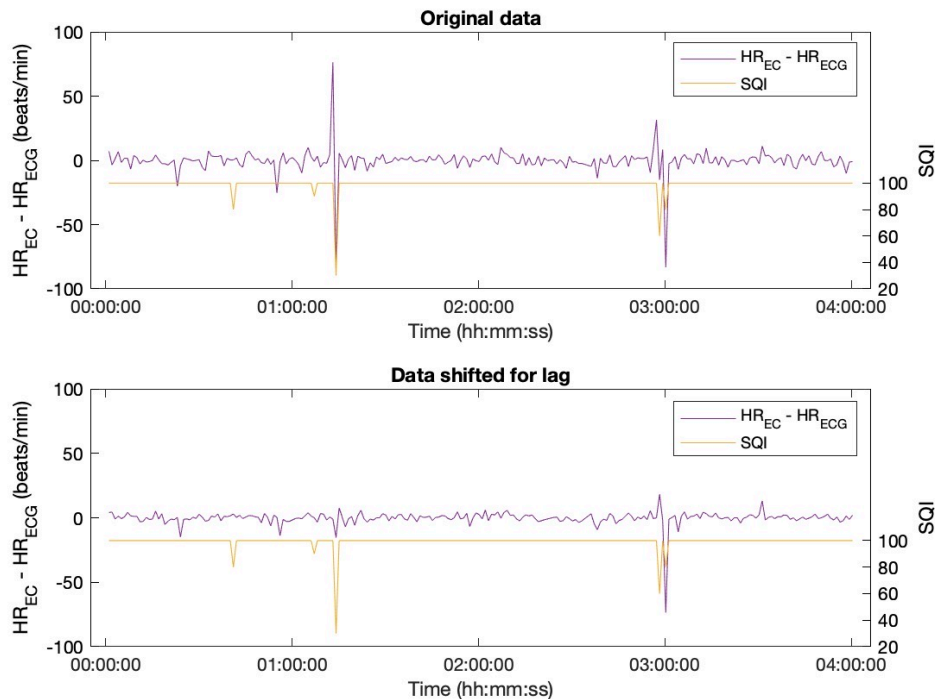


Figure 5.11: Difference between HR_{EC} and HR_{ECG} of a single patient over time. At the top, the original HR_{EC} and HR_{ECG} is shown. At the bottom, the HR_{ECG} data is shifted forward for the obtained lag of 1 minute.

5.5 Influence of patient weight and height

A significant strong positive linear correlation was found between CO_{EC} and patient weight, $r(41) = 0.78$, $p < 0.001$. Similar results were found for the correlation between CO_{EC} and patient height ($r(41) = 0.81$, $p < 0.001$). These correlations and the lines of regression are displayed in respective Figure 5.12 A and B. No correlation with the weight or height was found for LVO_{TTE} (Figure 5.12 C and D). RVO_{TTE} showed a weak insignificant correlation with both weight ($r = 0.27$, $p > 0.05$, Figure 5.12 E) and height ($r = 0.21$, $p > 0.05$, Figure 5.12 F). This indicates that the correlations of weight and height with RVO_{TTE} probably arose by chance.

5.6 Influence of transthoracic echocardiography

In Table 5.2 the results from the Friedman's ANOVA test are shown. Data of 41 measurements in 19 patients was assessed. Two measurements were removed from the dataset because EC measurements were concluded within one hour after the end of TTE. There was a statistically significant ($p = 0.014$) difference of the mean SQI before (median (IQR) = 91.7% (85.3 – 95.6)), during (86.4% (76.5 – 92.4)) and after TTE (90.5% (86.3 – 93.5)), with respective p-values of 0.016 and 0.002 between interval 2 and 1, and interval 2 and 3. This is also demonstrated by the percentage of data with a SQI below 70% ($p = 0.007$) and is visually presented in Figure 5.13. No clinically relevant or statistically significant difference between the three intervals was found for the mean SV ($p = 0.129$) and mean CO ($p = 0.518$). This indicates that even though the quality of the signal was affected by TTE, it did not alter the measured SV and CO by EC when the data was first filtered to remove data points with a SQI below 70%. Results of the post hoc tests for the COV of SV and CO showed a significantly lower percentage during interval 3 when compared to interval 1 ($p = 0.016$) and 2 ($p < 0.001$), indicating a more stable signal after performing TTE than before or during TTE.

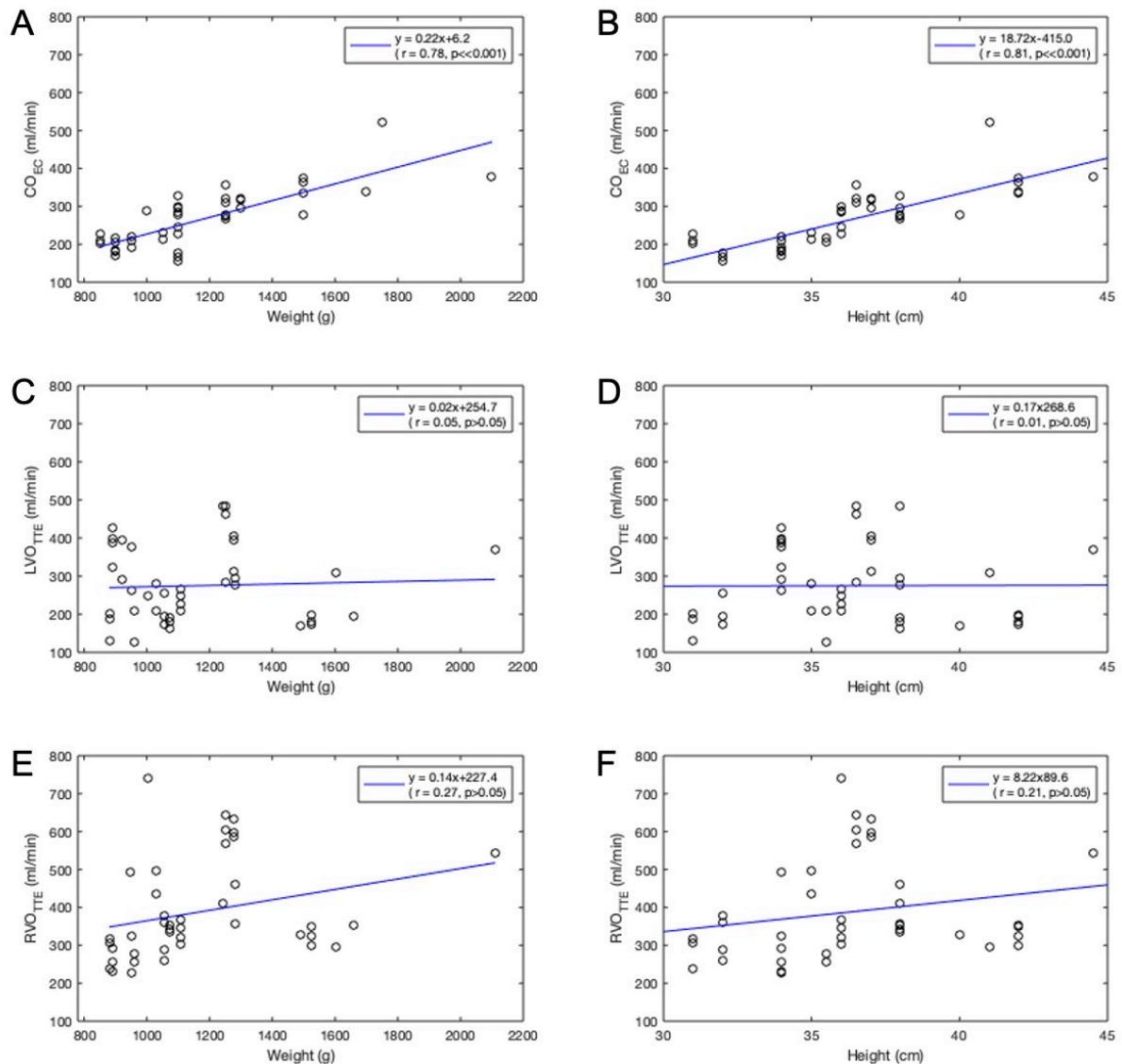


Figure 5.12: Correlations and lines of regression between patient weight or height and CO. A: weight vs CO_{EC} (N = 43); B: height vs CO_{EC} (N = 43); C: weight vs LVO_{TTE} (N = 43); D: height vs LVO_{TTE} (N = 43); E: weight vs RVO_{TTE} (N = 41); F: height vs RVO_{TTE} (N = 41).

A significant difference ($p < 0.001$) between the intervals was found for the mean HR with a moderate effect size of 0.329. For interval 1, 2, and 3 the median (IQR) of the mean HR was 166 (160 – 171), 166 (159 – 177), and 162 (154 – 169), respectively. Additionally, the range between maximum and minimum HR also differed between the intervals. During interval 1 the HR ranged from 106 to 188 beats/min, during interval 2 from 136 to 184 beats/min, and during interval 3 from 98 to 187 beats/min. This mainly shows a relatively similar maximum across all three intervals, but a significantly different ($p = 0.002$) minimum HR between the intervals. Overall, there was a lower mean and minimum HR after TTE when compared to during or before TTE, which can also be seen in Figure 5.13. It is noteworthy, however, that even though there was a significantly lower mean HR after TTE, the mean CO did not differ between the three intervals. This might be explained by the slight increase in mean SV during interval three. No clinically relevant or statistically significant difference was found between the intervals for any of the statistics of the SpO₂.

Table 5.2: Results of the Friedman's ANOVA tests with the effect size expressed by Kendall's W ($N = 41$). * $SQI < 70\%$

	Median			COV			Maximum			Minimum			% outliers		
SQI	$\chi^2(2)$	=	8.537	$\chi^2(2)$	=	7.657	$\chi^2(2)$	=	0.286	$\chi^2(2)$	=	0.286	$\chi^2(2)$	=	9.805*
	p	=	0.014	p	=	0.022		=	0.867	p	=	0.867	p	=	0.007*
	W	=	0.104	W	=	0.093	–	=	0.003	W	=	0.003	W	=	0.120*
SV	$\chi^2(2)$	=	4.098	$\chi^2(2)$	=	15.854	$\chi^2(2)$	=	4.327	$\chi^2(2)$	=	31.764	$\chi^2(2)$	=	12.634
	p	=	0.129	p	<	0.001	p	=	0.115	p	<	0.001	p	=	0.002
	W	=	0.050	W	=	0.193	W	=	4.327	W	=	0.387	W	=	0.154
CO	$\chi^2(2)$	=	1.317	$\chi^2(2)$	=	12.634	$\chi^2(2)$	=	5.899	$\chi^2(2)$	=	5.899	$\chi^2(2)$	=	12.847
	p	=	0.518	p	=	0.002	p	=	0.052	p	<	0.001	p	=	0.002
	W	=	0.016	W	=	0.154	W	=	0.072	W	=	0.302	W	=	0.157
HR	$\chi^2(2)$	=	26.976	$\chi^2(2)$	=	3.561	$\chi^2(2)$	=	15.753	$\chi^2(2)$	=	12.522	$\chi^2(2)$	=	2.098
	p	<	0.001	p	=	0.169	p	<	0.001	p	=	0.002	p	=	0.350
	W	=	0.329	W	=	0.043	W	=	0.192	W	=	0.153	W	=	0.026
SpO ₂	$\chi^2(2)$	=	2.390	$\chi^2(2)$	=	1.024	$\chi^2(2)$	=	3.758	$\chi^2(2)$	=	4.271	$\chi^2(2)$	=	0.634
	p	=	0.303	p	=	0.599	p	=	0.153	p	=	0.118	p	=	0.728
	W	=	0.029	W	=	0.012	W	=	0.046	W	=	0.052	W	=	0.008

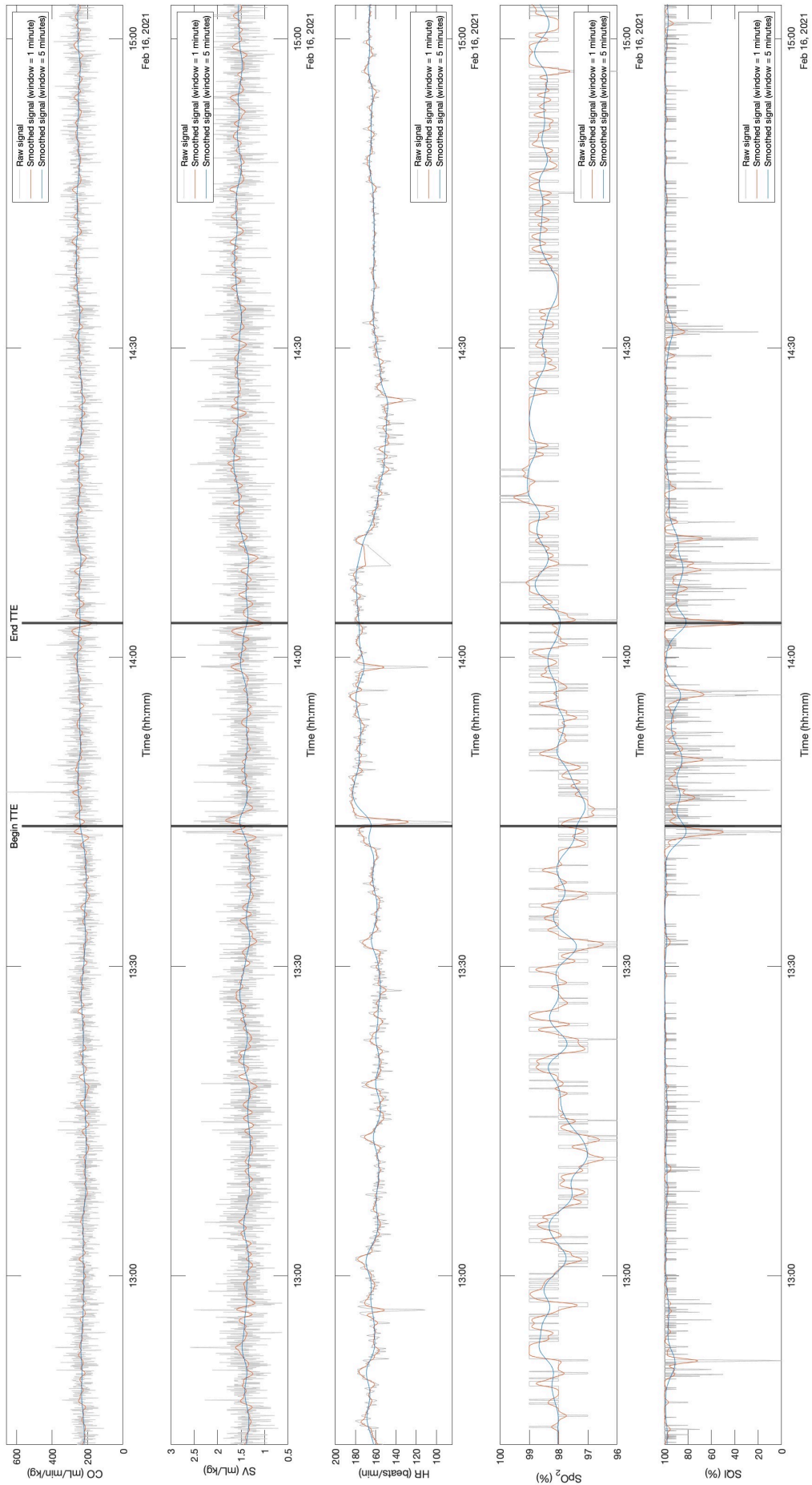


Figure 5.13: Measured parameters of a single patient for the three intervals; before, during, and after TTE.

5.7 Usability

The results of the assessment of electrode durability are depicted in Figure 5.14. In this figure, the proportion of samples with a good SQI is shown over time for three subjects, whose results are representative for all included patients. At the top of Figure 5.14, the results of a subject who was connected to the electrical cardiometer for 140 hours are shown. After approximately 50 hours of measurement the proportion of samples with a good SQI starts decreasing and after 90 hours the SQI becomes significantly worse. However, in another subject the percentage of data with a good SQI remained high until the end of the measurement after approximately 100 hours (Figure 5.14, middle). Similar results were found for a subject who was connected to the cardiometer for 200 hours (Figure 5.14, bottom) where the SQI remained high until 130 hours after which it gradually started decreasing but still within acceptable limits. These data suggest that the durability of the electrodes varies considerably among patients, making it impossible to define an exact durability of the electrodes.

Besides evaluation of the SQI over time, electrode durability was also assessed by how long the electrodes remained adhered to the skin. After exclusion of the subjects for whom the measurement was discontinued due to discharge from the NICU, six subjects remained. In these subjects, the electrodes remained adhered for a median (IQR) time of 79.5 (64 – 129) hours with a minimum of 62 and maximum of 213 hours. This large range between subjects may be caused by several factors, such as the humidity of the incubator, the patient's skin, and patient movement.

Other aspects for judging the usability of EC were the duration of calibration, application and interpretation of the user interface, and the ability to record the data along with the other haemodynamic parameters. At the start of a measurement, the electrical cardiometer auto-calibrates itself within less than a minute. The user interface is easy to apply, and it is possible to choose an averaging mode for the measurands. This makes interpretation of the CO easier for the physician, as offline filtering of the data is not necessary. The SQI is shown at the top of the screen to show the user whether the reported values are reliable. Multiple screens are available which show the value of the measurands as well as the CO and HR over time. Recording of the data along with the other haemodynamic parameters is possible through connection with the Philips IntelliVue monitor. A disadvantage is that the CO is expressed in L/min and it is indexed for body surface area, whereas in neonates mL/min and indexing for body weight is preferred.

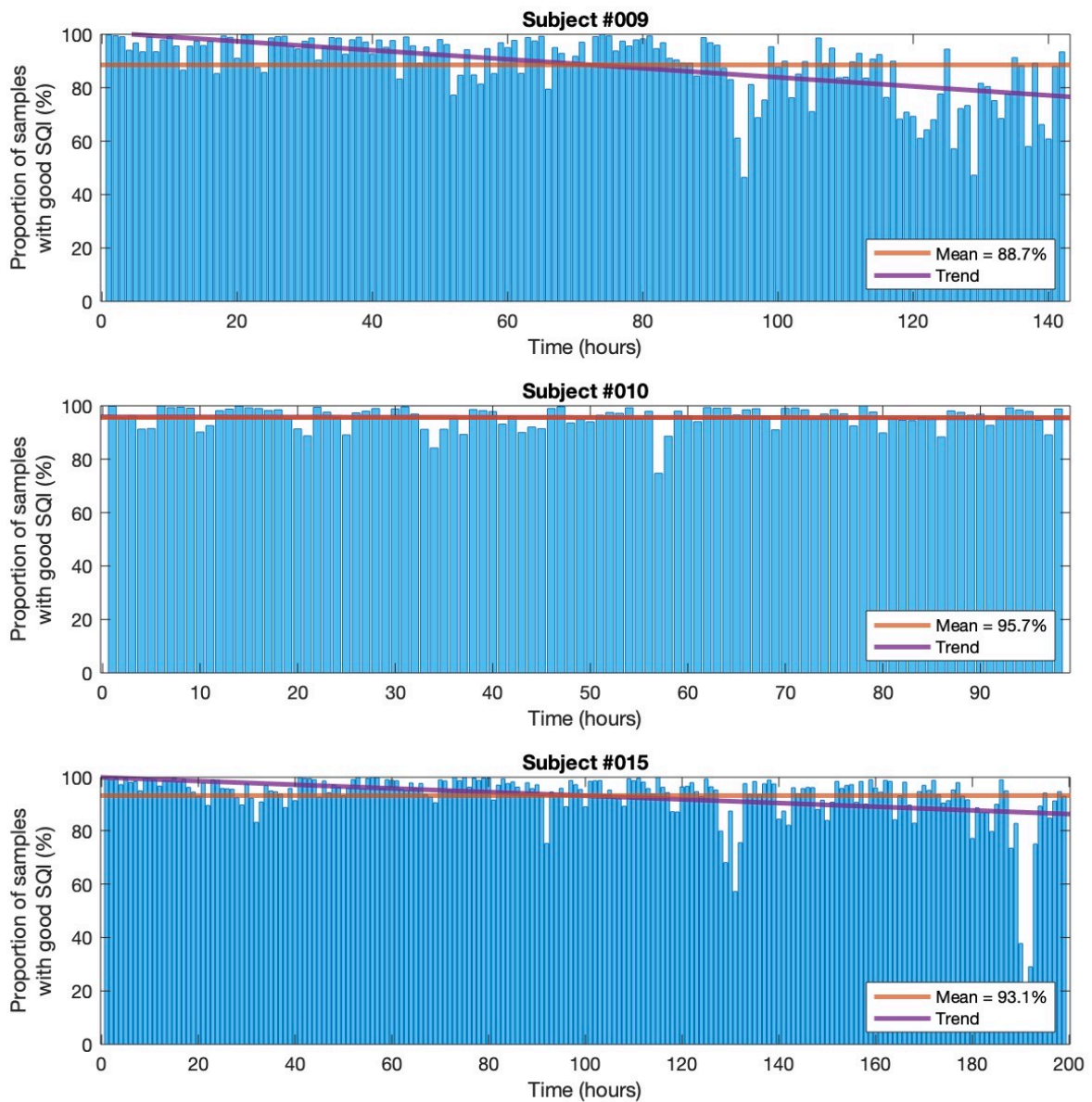


Figure 5.14: The proportion of samples with a good SQI ($\geq 70\%$) over time shown for three individual subjects.

6 DISCUSSION

In this study the accuracy, reliability, and applicability of EC for monitoring the CO in NICU patients was investigated. When comparing CO_{EC} with LVO_{TTE} and RVO_{TTE} , CO_{EC} appears to agree more with RVO_{TTE} than LVO_{TTE} . The bias%, corrected error%, similar categorisation percentage, angular bias, and radial LOA of CO_{EC} compared with RVO_{TTE} were found to be -32.9%, 55.9%, 63.4%, -23.6°, and $\pm 60^\circ$, respectively. For the comparison with LVO_{TTE} , this was respective -8%, 81.6%, 58.1%, -29.5°, and $\pm 60^\circ$. However, the bias between CO_{EC} and RVO_{TTE} was relatively large, indicating that EC underestimates RVO. Performance of TTE did not influence the reliability of CO_{EC} . During TTE, there was a lower mean SQI (86.4%) than before (91.7%) or after (90.5%) TTE, but this did not affect the CO_{EC} used for the assessment of agreement and trending between EC and TTE. Nevertheless, the high error%, low concordance rate (55.5% for LVO and 50% for RVO) and high angular bias with wide angular LOA demonstrate that the EC is not interchangeable with TTE.

6.1 Validation and trending ability of electrical cardiometry

For EC to be interchangeable with TTE, the error% should have been below 30%, according to the critical limit for acceptance as proposed by Critchley & Critchley[28]. However, this limit is disputable as it is based on a reference method with a 20% error. Adjusting the error% for the 30% error of TTE results in a critical limit for acceptance of agreement of 42.4% (error% $_{EC+TTE}$), i.e. EC could have been accepted as a good method for measuring cardiac output if its error% was less or similar to the 30% error of TTE.[29] Peyton and Chong[33] suggest increasing the limit of error% from 30 to 45% because their meta-analysis showed that the error% of several CO monitoring methods was between 40 and 45% when compared with thermodilution (error% 10-20%). But, with increasing the limit of acceptable error%, there is a risk of wrongfully declaring a new method as interchangeable with the reference method. The high error% found in this study, therefore, makes it impossible to accept EC as a good method for CO measurement. In other studies investigating the agreement between CO_{EC} and LVO_{TTE} , high error% were reported as well with the error% ranging from 24 to 60.2%.[21, 23, 24, 34] Ideally, the error% of a new method is as low as possible where the bias% is of less importance as a method can be calibrated for a low accuracy (systematic error) but not for a low precision.

A large difference between LVO_{TTE} and RVO_{TTE} , 244 vs 335 mL/min/kg, was found in this study. No literature was found reporting similar differences as most studies only address the LVO. One study reported a mean LVO and RVO of 218 and 227 mL/min/kg, respectively, in 40 preterm neonates.[24] A possible explanation for the difference between LVO_{TTE} and RVO_{TTE} in our study is that the LVO is technically more difficult to measure than the RVO. This may have caused a larger deviation from the ideal angle of insonation resulting in an underestimation of the LVO.

In 18.6% of the comparative data EC overestimated LVO, which might suggest that EC is incapable to detect low CO. This was also reported by Song et al. [24], where no correlation was found between CO_{EC} and LVO or RVO in infants with a CO below 200 mL/min/kg. Theoretically, decreased blood flow in the thorax while in a low CO state may have had a diminishing effect on the signal-to-noise ratio of EC. In other words, the EC signal might be more severely disrupted by noise in a low CO state than in a normal or high CO state, making it impossible to give a correct reading of the CO. Another possibility is that the limitations of TTE resulted in erroneous CO measurements, causing a wrong categorization of the LVO and RVO. Both underestimation and overestimation of the CO could be harmful to the patient. If the CO is overestimated, hypoperfusion and shock may not be recognized in time which can increase the risk of patient morbidity and mortality, whereas underestimation of the CO may lead to unnecessary therapeutic interventions.

In respective 23.3% and 36.6% of the cases EC underestimated LVO and RVO. This might have been caused by intra- and extracardiac shunts, where systemic blood flow is overestimated by RVO_{TTE} in the case of left-to-right shunting through a PFO and by LVO_{TTE} in the case of left-to-right shunting through a PDA. It is uncertain if EC measures the blood flow preductally, postductally, or both. Theoretically, EC reflects changes in blood flow in any vessel parallel to the distance between the electrodes on the neck and thorax, which implies that it cannot distinguish pre- and postductal blood flow. Since the size of this study population was small, no distinction was made for the presence of a PDA or PFO. Results from studies investigating the influence of a haemodynamically significant PDA with a left-to-right shunt are inconclusive. Song et al. [24] describe a correlation between EC and TTE that is independent of the presence of a PDA. In addition, Noori et al. [21] reported no difference in bias and error% between patients with or without a PDA. On the other hand, Torigoe et al. [35] state that there was a larger negative bias in patients with a PDA, whereas Blohm et al. [34] describe a significant positive increase in bias. Therefore, no clear conclusion can be drawn as to whether EC is accurate in neonates with a PDA and/or PFO.

The concordance analysis showed that the range of ΔLVO_{TTE} and ΔRVO_{TTE} was twice as large as the range of ΔCO_{EC} . This could indicate that either TTE is showing false differences between measurements due to its high intra- and interobserver variability or that the CO of the patients did change but that it was not registered by EC. Therefore, the disagreement between EC and TTE and the poor trending could be induced by incorrect measurements of either method. One could argue that CO measured with TTE is correct since the reference method should be valid. However, the limitations of echocardiography make this a subject of discussion. For example, when analysing the data, it was found that the diameter of the LVOT and RVOT showed an unrealistic variation between measurements. In Figure 3 and 4 of Appendix 8 the diameters of the aorta and the PA are shown, respectively. Due to the unrealistic variation, the measured diameters within a single patient were averaged for the calculation of CO.

6.2 Reliability

Inspection of the equations used by EC to calculate SV and CO raised some questions. First of all, the model was created based on adults which may very well not be sufficient for neonates. Second, when going from acceleration to velocity (section 2.3.2 equation 2.2), a square root is used to derive the velocity from the peak acceleration instead of integrating the acceleration. According to the manufacturer, this can be justified because they found that using the square root to calculate the velocity is sufficient to approximate the cardiac output. Third, there was a strong significant correlation between CO_{EC} and patient weight ($r = 0.78$, $p < 0.001$) and height ($r = 0.84$, $p < 0.001$), whereas a none-to-weak correlation was found for LVO_{TTE} and RVO_{TTE} .

A certain correlation between CO and weight was expected, because in neonates CO physiologically increases with weight which is why CO is generally normalized for bodyweight in this population. However, since LVO_{TTE} and RVO_{TTE} showed none-to-weak correlation while CO_{EC} showed strong correlation with patient weight, it is arguable that EC perhaps relies too heavily on the entered weight and height for the calculation of SV and CO (section 2.3.2 equation 2.4).

Furthermore, comparison of HR_{EC} with HR_{ECG} showed that the methods are interchangeable and the time lag that existed between the two methods is clinically irrelevant. The bias% and error% of SV_{EC} and CO_{EC} in this study were found to be comparable. Similar findings were reported in a recent study by Schwarz et al.³⁷ in neonates with a median (IQR) gestational age of 28+6 (24+5 – 30+4) weeks + days and a birth weight of 890 (723 – 1335) g. This indicates that if EC miscalculates the CO, this mistake can be traced back to the calculation of SV instead of the measured HR.

6.3 Usability

The usability of EC was found to be good, considering it provides continuous assessment of the CO and CO is recordable along with the other haemodynamic parameters. Moreover, EC was experienced as practical, and easy to apply and interpret. Results of the analysis of EC electrode durability showed that it is not necessarily required to replace the electrodes after 72 hours of EC, as is advised by the manufacturer. The proportion of samples with a good SQI ($SQI \geq 70\%$) over time differed among patients. Some patients showed a low percentage of data with good SQI even within the first 72 hours of EC, whereas in others the SQI was still high after 100 hours of measuring. It is therefore suggested to only replace the electrodes when the SQI remains below 70% for more than fifteen minutes or when the electrodes detached from the skin. Besides, the electrodes mostly adhered firmly to the patients' skin, making it unpleasant for the patients to remove them earlier than necessary.

6.4 Limitations

This study has several limitations. First, only haemodynamically stable patients were included in which a normal CO was expected. The results of this study are, therefore, internally valid for this population, but not externally valid for for example term neonates or haemodynamically instable patients. To achieve external validation, the patient population should be extended to also include less clinically stable infants with a low or high CO. Secondly, TTE was used as a reference method even though it has significant limitations as mentioned before. Since thermodilution, which is considered the gold standard in adults, cannot be used in neonates due to technical limitations, TTE is often reported in literature as reference method for validation of electrical biosensing technologies. Third, the aim was to conduct TTE once per day to assess trending ability but due to other proceedings it simply was impossible to perform TTE every day in every patient.

It is important to mention that even if a noninvasive CO monitor is to be used in the future, TTE will always need to be performed at least once to assess the anatomy and pathophysiology of the patient's heart and cardiovascular status. Additionally, to assess the haemodynamic state of a patient, the CO on its own is not reliable. The other haemodynamic parameters always need to be taken into consideration before interfering. Besides, CO only provides information on systemic blood flow, but not on local perfusion and oxygenation. If information on local oxygenation is required, near-infrared spectroscopy may be used.

7 CONCLUSION

The main goal of this study was to determine the accuracy, reliability, and applicability of EC. Agreement and trending between EC and TTE was poor, hence EC and TTE are not interchangeable. The bias% (accuracy) of CO_{EC} , when compared with LVO_{TTE} , was found to be -8% with an error % of 81.6%. When compared with RVO_{TTE} , the bias% was -32.9% and the error% 55.9%. Assessment of the trending ability of EC showed concordance rates of 55.5% (LVO_{TTE}) and 50% (RVO_{TTE}), and angular biases of -29.5° (LVO_{TTE}) and -23.6° (RVO_{TTE}). However, due to the limitations of TTE, it is unclear to what extent the disagreement between the two methods is caused by erroneous CO measurements by either EC or TTE, which emphasizes the need for another, more accurate and reliable reference method.

Performance of TTE did not influence the reliability of CO_{EC} , but the strong significant correlation found between CO_{EC} and patient weight ($r = 0.78$, $p < 0.001$) and height ($r = 0.84$, $p < 0.001$) raised some questions on the calculation of CO_{EC} and the extent to which it relies on the patient weight and height.

To conclude, even though EC showed good usability, the accuracy and reliability of EC for measuring CO is poor, deeming EC not applicable yet to monitor CO in critically ill newborns.

8 RECOMMENDATIONS AND FUTURE WORK

Based on the results of the validity and trend analysis, EC cannot be recommended for CO monitoring on the NICU for now. More research with an accurate reference method is necessary, as well as extending the population to also include haemodynamically unstable patients.

For further research into CO monitoring on the NICU, it is recommended to first investigate the influence of the weight and height on CO_{EC} more extensively. For example, a test could be run to see whether CO_{EC} in a haemodynamically stable patient changes when the weight or the height is adjusted on the cardiometer. If the calculation of CO_{EC} is highly dependable on the weight and height, this would induce an increase in CO upon increasing the entered weight or height. Additionally, it could be considered to validate EC based on our knowledge of (patho)physiology. Neonates in which a low CO is expected can be included, for example patients receiving therapeutic hypothermia for perinatal asphyxia, as well as patients with an expected high CO (e.g. vasoplegia). Moreover, trending ability of EC could be assessed during rewarming after therapeutic hypothermia which will cause an increase in CO.

A more accurate technique to measure CO and which could therefore be used as a reference method in future studies, is transpulmonary ultrasound dilution (TPUD). With TPUD, an arteriovenous (AV) loop is placed between the arterial and central venous catheter and 0.5 to 1.0 mL/kg isotonic saline at body temperature is injected at the venous side of the AV loop. Since sound waves propagate slower through saline (1533 m/s) than blood (1560 – 1580 m/s), a decreased ultrasound velocity is measured downstream at the arterial side of the AV loop. As the altering concentration of isotonic saline over time is related to CO, the resulting ultrasound dilution curve can be used to calculate CO with the Stewart-Hamilton equation. An important limitation of TPUD is the requirement of isotonic saline injections. Repeated measures with TPUD will increase the risk of fluid overload, especially in neonates, which is associated with an increased risk of PDA and necrotizing enterocolitis. TPUD is possible in infants weighing over 600 g.[\[12, 29, 36, 37\]](#)

Another reference method might be 3-dimensional (3D) echocardiography. In this method a dedicated 3D probe is used to make a recording of the four-chamber view. End-diastolic and end-systolic volume can be determined offline using a software program with semi-automated endocardial border detection. CO can be calculated by multiplying the difference between end-diastolic and end-systolic volume with the HR.[\[38\]](#)

A different noninvasive electrical biosensing technology to measure CO could be investigated as well, such as the Starling SV or the NICaS. The Starling SV uses a method called transthoracic bioimpedance to calculate the CO. Transthoracic bioimpedance has been validated against thermodilution in adults, giving a bias% of 4.1% and an error% of 11.3%, along with a 93% sensitivity and specificity to detect hemodynamic changes.[\[39\]](#) In children and neonates validation studies have been performed using TTE, with reported bias% and error% ranging from 4.6 to 39% and 31.4 to 55%, respectively.[\[40, 41, 42, 43, 44\]](#) The NICaS uses whole-body bioimpedance to calculate the CO. Validation studies of whole-body bioimpedance have been performed in adults

with thermodilution, Fick principle, and TTE as reference methods. Bias% and error% were stated to range from 0.2 to 12.3% and 20.0 to 48.1%, respectively. [45, 46, 47, 48, 49] Only one study reported the validation of whole-body bioimpedance in children, showing a bias% of 1.8% and an error% of 29.4%, with transoesophageal doppler as reference method. [50] No validation studies of whole-body bioimpedance in neonates have been published yet.

REFERENCES

- [1] Kathryn N. Ivey and Deepak Srivastava. The paradoxical patent ductus arteriosus, 2006.
- [2] Nandan S. Anavekar and Jae K. Oh. Doppler echocardiography: A contemporary review. *Journal of Cardiology*, 54(3):347–358, 2009.
- [3] Willem P. de Boode, Robin van der Lee, Beate Horsberg Eriksen, Eirik Nestaas, Eugene Dempsey, Yogen Singh, Topun Austin, and Afif El-Khuffash. The role of Neonatologist Performed Echocardiography in the assessment and management of neonatal shock, 2018.
- [4] Markus Osypka. An Introduction to Electrical Cardiometry™. *Electrical Cardiometry™*, 49(6):1–10, 2009.
- [5] Zorg rond de geboorte | Cijfers & Context | Gebruik | Volksgezondheidszorg.info.
- [6] Shane M. Tibby, Mark Hatherill, Michael J. Marsh, and Ian A. Murdoch. Clinicians' abilities to estimate cardiac index in ventilated children and infants. *Archives of Disease in Childhood*, 77(6):516–518, 1997.
- [7] Jonathan G. Bensley, Robert De Matteo, Richard Harding, and Mary J. Black. The effects of preterm birth and its antecedents on the cardiovascular system. *Acta Obstetrica et Gynecologica Scandinavica*, 95(6):652–663, 2016.
- [8] Matthew McGovern and Jan Miletin. Cardiac output monitoring in preterm infants. *Frontiers in Pediatrics*, 6(April):1–10, 2018.
- [9] Sabine L. Vrancken, Arno F. van Heijst, and Willem P. de Boode. Neonatal Hemodynamics: From developmental physiology to comprehensive monitoring. *Frontiers in Pediatrics*, 6(April):1–15, 2018.
- [10] Ronald I. Clyman, James Couto, and Gail M. Murphy. Patent Ductus Arteriosus: Are Current Neonatal Treatment Options Better or Worse Than No Treatment at All?, 4 2012.
- [11] Tai Wei Wu, Timur Azhibekov, and Istvan Seri. Transitional hemodynamics in preterm neonates: Clinical relevance. *Pediatrics and Neonatology*, 57(1):7–18, 2016.
- [12] Willem Pieter de Boode. Advanced Hemodynamic Monitoring in the Neonatal Intensive Care Unit, 2020.
- [13] Prince & Links, Medical Imaging Signals and Systems, 2nd Edition | Pearson.
- [14] Koert De Waal, Martin Kluckow, and Nick Evans. Weight corrected percentiles for blood vessel diameters used in flow measurements in preterm infants. *Early Human Development*, 89(12):939–942, 2013.
- [15] M. S. Chew and J. Poelaert. Accuracy and repeatability of pediatric cardiac output measurement using Doppler: 20-Year review of the literature. *Intensive Care Medicine*, 29(11):1889–1894, 2003.

- [16] C. Schmidt, G. Theilmeier, H. Van Aken, P. Korsmeier, S. P. Wirtz, E. Berendes, A. Hoffmeier, and A. Meissner. Comparison of electrical velocimetry and transoesophageal Doppler echocardiography for measuring stroke volume and cardiac output. *British Journal of Anaesthesia*, 95(5):603–610, 2005.
- [17] ICON ® NONINVASIVE HEMODYNAMICS Electrical Cardiometry™. Technical report, Osypka Medical GmbH, 2014.
- [18] Electrical Cardiometry Technology (EC) | Osypka Medical | Cardiotronic.
- [19] Osypka MJ. Bernstein DP. Apparatus and method for determining an approximation of the stroke volume and the cardiac output of the heart. *US Patent 6,511,438 B2, January 28, 2003*, 2(12), 2003.
- [20] Jitin Narula, Sandeep Chauhan, Sivasubramanian Ramakrishnan, and Saurabh Kumar Gupta. Electrical Cardiometry: A Reliable Solution to Cardiac Output Estimation in Children With Structural Heart Disease. *Journal of Cardiothoracic and Vascular Anesthesia*, 2017.
- [21] Shahab Noori, Benazir Drabu, Sadaf Soleymani, and Istvan Seri. Continuous non-invasive cardiac output measurements in the neonate by electrical velocimetry: A comparison with echocardiography. *Archives of Disease in Childhood: Fetal and Neonatal Edition*, 2012.
- [22] Ralf Rauch, Eva Welisch, Nathan Lansdell, Elizabeth Burrill, Judy Jones, Tracy Robinson, Dirk Bock, Cheril Clarson, Guido Filler, and Kambiz Norozi. Non-invasive measurement of cardiac output in obese children and adolescents: Comparison of electrical cardiometry and transthoracic Doppler echocardiography. *Journal of Clinical Monitoring and Computing*, 27(2):187–193, 4 2013.
- [23] Oswin Grollmuss and Patricia Gonzalez. Non-invasive cardiac output measurement in low and very low birth weight infants: A method comparison. *Frontiers in Pediatrics*, 2014.
- [24] R. Song, W. Rich, J. H. Kim, N. N. Finer, and A. C. Katheria. The use of electrical cardiometry for continuous cardiac output monitoring in preterm neonates: a validation study. *American journal of perinatology*, 31(12):1105–1110, 12 2014.
- [25] A. Boet, G. Jourdain, S. Demontoux, and D. De Luca. Stroke volume and cardiac output evaluation by electrical cardiometry: Accuracy and reference nomograms in hemodynamically stable preterm neonates. *Journal of Perinatology*, 36(9):748–752, 9 2016.
- [26] Silvia Martini, Giulia Frabboni, Paola Rucci, Marek Czosnyka, Peter Smielewski, Silvia Galletti, Anna Giulia Cimatti, Giacomo Faldella, Luigi Corvaglia, and Topun Austin. Cardiovascular and cerebrovascular responses to cardio-respiratory events in preterm infants during the transitional period. *Journal of Physiology*, 2020.
- [27] S. Soleymani, I. Seri, and I. Seri. Hemodynamic monitoring in neonates: Advances and challenges. *Journal of Perinatology*, 30(S1):S38–S45, 2010.
- [28] Lester A.H. Critchley and Julian A.J.H. Critchley. A meta-analysis of studies using bias and precision statistics to compare cardiac output measurement techniques. *Journal of Clinical Monitoring and Computing*, 1999.
- [29] Willem Pieter de Boode, Markus Osypka, S. Soleymani, and Shahab Noori. Assessment of cardiac output in neonates: techniques using the Fick principle, indicator dilution technology, Doppler ultrasound, thoracic electrical impedance, and arterial pulse contour analysis. In Richard A. Polin, editor, *Hemodynamics and Cardiology*, chapter 14, pages 237–263. Elsevier, Inc., 3rd edition, 2019.

- [30] Lester A. Critchley, Xiao X. Yang, and Anna Lee. Assessment of trending ability of cardiac output monitors by polar plot methodology. *Journal of Cardiothoracic and Vascular Anesthesia*, 25(3):536–546, 2011.
- [31] Lester A. Critchley, Anna Lee, and Anthony M.H. Ho. A critical review of the ability of continuous cardiac output monitors to measure trends in cardiac output. *Anesthesia and Analgesia*, 111(5):1180–1192, 2010.
- [32] Ellen Marshall and Basile Marquier. Friedman test in SPSS.
- [33] P. J. Peyton and S. W. Chong. Minimally invasive measurement of cardiac output during surgery and critical care: A meta-analysis of accuracy and precision (Anesthesiology (2010) 113, (1220-1235)). *Anesthesiology*, 116(4):973, 2012.
- [34] Martin Ernst Blohm, Jana Hartwich, Denise Obrecht, Jan Felix Kersten, and Dominique Singer. Effect of patent ductus arteriosus and patent foramen ovale on left ventricular stroke volume measurement by electrical velocimetry in comparison to transthoracic echocardiography in neonates. *Journal of Clinical Monitoring and Computing*, 31(3):589–598, 2017.
- [35] T. Torigoe, S. Sato, Y. Nagayama, T. Sato, and H. Yamazaki. Influence of patent ductus arteriosus and ventilators on electrical velocimetry for measuring cardiac output in very-low/low birth weight infants. *Journal of Perinatology*, 35(7):485–489, 2015.
- [36] S. L. Vrancken, W. P. De Boode, J. C. Hopman, S. K. Singh, K. D. Liem, and A. F. Van Heijst. Cardiac output measurement with transpulmonary ultrasound dilution is feasible in the presence of a left-to-right shunt: A validation study in lambs. *British Journal of Anaesthesia*, 2012.
- [37] Willem P. De Boode, Arno F.J. Van Heijst, Jeroen C.W. Hopman, Ronald B. Tanke, Hans G. Van Der Hoeven, and Kian D. Liem. Cardiac output measurement using an ultrasound dilution method: A validation study in ventilated piglets. *Pediatric Critical Care Medicine*, 2010.
- [38] Stephen P Hoole, James Boyd, Vlasis Ninios, Jayan Parameshwar, and Rosemary A Rusk. Measurement of cardiac output by real-time 3D echocardiography in patients undergoing assessment for cardiac transplantation.
- [39] Nirav Y. Raval, Pierre Squara, Michael Cleman, Kishore Yalamanchili, Michael Winklmaier, and Daniel Burkhoff. Multicenter evaluation of noninvasive cardiac output measurement by bioreactance technique. *Journal of Clinical Monitoring and Computing*, 2008.
- [40] Dany E. Weisz, Amish Jain, Patrick J. McNamara, and Afif EL-Khuffash. Non-Invasive Cardiac Output Monitoring in Neonates Using Bioreactance: A Comparison with Echocardiography. *Neonatology*, 102(1):61–67, 6 2012.
- [41] Dany E. Weisz, Amish Jain, Joseph Ting, Patrick J. McNamara, and Afif El-Khuffash. Non-invasive cardiac output monitoring in preterm infants undergoing patent ductus arteriosus ligation: A comparison with echocardiography. *Neonatology*, 106(4):330–336, 11 2014.
- [42] Estelle Vergnaud, Charles Vidal, Juliette Montmayeur Verchere, Hanna Taright, Philippe G. Meyer, Pierre A. Carli, and Gilles A. Orliaguet. Noninvasive cardiac output measurement using bioreactance in postoperative pediatric patients. *Paediatric Anaesthesia*, 25(2):160–166, 2 2015.

- [43] Ying Sun, Chi Wu, Jun-Zheng Wu, Shan-Shan Wang, Jie Bai, Ming Zhu, Yu-Qi Zhang, and Ma-Zhong Zhang. Noninvasive cardiac output monitoring using bioactance-based technique in pediatric patients with or without ventricular septal defect during anesthesia: in comparison with echocardiography. *Pediatric Anesthesia*, 25(2):167–173, 2 2015.
- [44] Eva Forman, Colm R. Breatnach, Stephanie Ryan, Jana Semberova, Jan Miletin, Adrienne Foran, and Afif El-Khuffash. Noninvasive continuous cardiac output and cerebral perfusion monitoring in term infants with neonatal encephalopathy: Assessment of feasibility and reliability. *Pediatric Research*, 2017.
- [45] Amram J. Cohen, Dimitri Arnaudov, Deeb Zabeeda, Lex Schultheis, John Lashinger, and Arie Schachner. Non-invasive measurement of cardiac output during coronary artery by-pass grafting. *European Journal of Cardio-thoracic Surgery*, 1998.
- [46] Gad Cotter, Yaron Moshkovitz, Edo Kaluski, Amram J. Cohen, Hilton Miller, Daniel Goor, and Zvi Vered. Accurate, noninvasive continuous monitoring of cardiac output by whole-body electrical bioimpedance. *Chest*, 2004.
- [47] Oscar Luis Paredes, Junya Shite, Toshiro Shinke, Satoshi Watanabe, Hiromasa Otake, Daisuke Matsumoto, Yusuke Imuro, Daisuke Ogasawara, Takahiro Sawada, and Mitsuhiro Yokoyama. Impedance cardiography for cardiac output estimation - Reliability of wrist-to-ankle electrode configuration. *Circulation Journal*, 70(9):1164–1168, 2006.
- [48] Yu Taniguchi, Noriaki Emoto, Kazuya Miyagawa, Kazuhiko Nakayama, Hiroto Kinutani, Hidekazu Tanaka, Toshiro Shinke, and Ken Ichi Hirata. Noninvasive and simple assessment of cardiac output and pulmonary vascular resistance with whole-body impedance cardiography is useful for monitoring patients with pulmonary hypertension. *Circulation Journal*, 2013.
- [49] Michael J. Germain, Jyovani Joubert, Daniel O’Grady, Brian H. Nathanson, Yossi Chait, and Nathan W. Levin. Comparison of stroke volume measurements during hemodialysis using bioimpedance cardiography and echocardiography. *Hemodialysis International*, 22(2):201–208, 2018.
- [50] R. Beck, L. Milella, and C. Labellarte. Continuous non-invasive measurement of stroke volume and cardiac index in infants and children: comparison of Impedance Cardiography NICaS® vs CardioQ® method. *La Clinica terapeutica*, 2018.

APPENDIX A: FIGURES

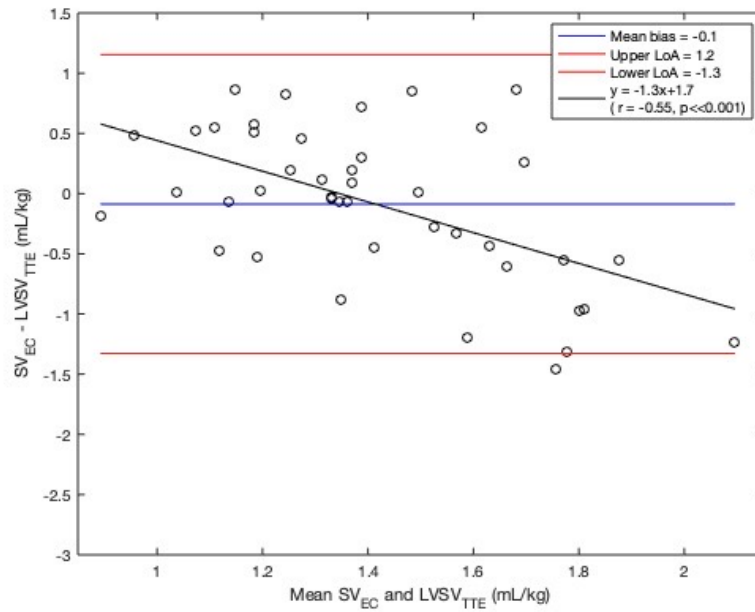


Figure 1: Bland-Altman analysis of SV_{EC} and LVSV_{TTE} (N = 43).

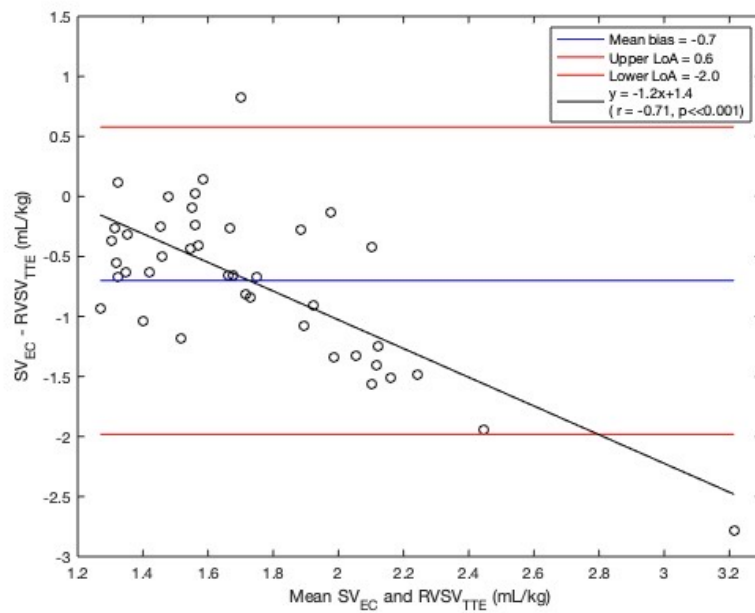


Figure 2: Bland-Altman analysis of SV_{EC} and RSV_{TTE} (N = 41).

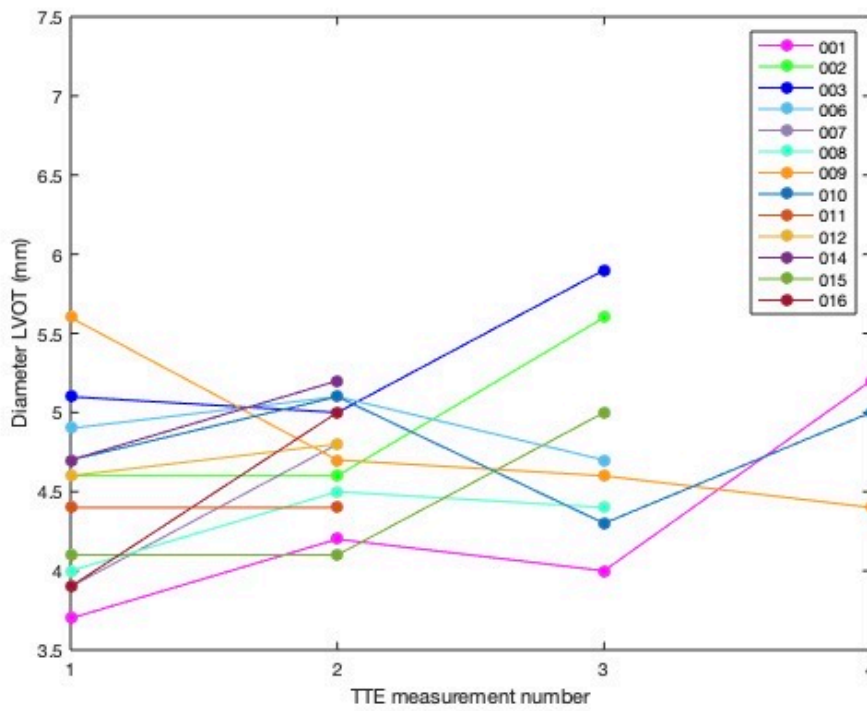


Figure 3: Measured diameter of the LVOT at the hinge points of the aortic valve in patients where multiple TTE's were performed (N = 13).

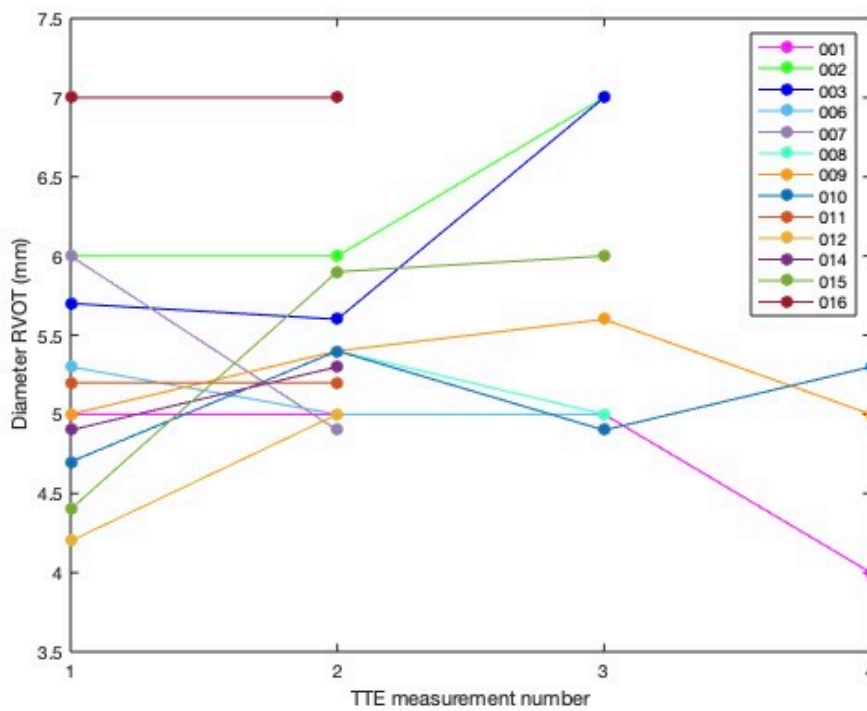


Figure 4: Measured diameter of the RVOT at the pulmonary valve insertion in patients where multiple TTE's were performed (N = 13).

APPENDIX B: TABLES

Table 1: Results of the Bland-Altman analyses of HR_{EC} and HR_{ECG} (N = 19).

	Mean bias (beats/min)	SD of bias (beats/min)	Bias% (%)	Error% (%)
Mean	-0.12	9.5	-0.041	5.9
SD	0.54	3.2	0.18	2.0
Minimal	-1.1	3.8	-0.41	2.3
Maximal	0.77	17	0.25	9.9

Table 2: Results of the Bland-Altman analyses of HR_{EC} and HR_{ECG}, with HR_{ECG} shifted for the time lag (N = 19).

	Mean bias (beats/min)	SD of bias (beats/min)	Bias% (%)	Error% (%)
Mean	-0.011	8.3	-0.0023	5.2
SD	0.61	3.5	0.20	2.4
Minimal	-1.1	3.8	-0.43	2.3
Maximal	0.88	15	0.32	10.9